the efficiency of packing decreases upon melting; the effective hard-core volume increases, decreasing the free volume. Thus, the constant-volume contribution to the entropy should be less than that due to chain conformations alone. This is consistent with the conclusion drawn by Robertson from heat capacity and equation of state measurements on poly(methylene) glasses, from which conformational and constant-volume entropies can be independently estimated.[36] In constant-pressure melting, on the other hand, the increase in volume is predicted to be greater than the increase in hard-core volume; thus the free volume will increase and the conformational entropy is an underestimate of the constant-pressure entropy of fusion.

Registry No. Polyethylene (homopolymer), 9002-88-4.

References and Notes

(1) Müller, A. *Proc. R. Soc. London, A* **1932**, *138*, 514.
(2) Doucet, J.; Denicolo, I.; Craievich, A. *J. Chem. Phys.* **1981**, *75*, 1523.
(3) Doucet, J.; Denicolo, I.; Craievich, A.; Collet, A. *J. Chem. Phys.* **1981**, *75*, 5125.
(4) Denicolo, I.; Doucet, J.; Craievich, A. *J. Chem. Phys.* **1983**, *78*, 1465.
(5) Doucet, J.; Denicolo, I.; Craievich, a.; Germain, C. *J. Chem. Phys.* **1984**, *80*, 1647.
(6) Ungar, G. *J. Phys. Chem.* **1983**, *87*, 689.
(7) Flory, P. J.; Orwoll, R. A.; Vrij, A. *J. Am. Chem. Soc.* **1964**, *86*, 3507.
(8) Broadhurst, M. G. *J. Res. Natl. Bur. Stand., Sect. A* **1962**, *66A*, 241; *J. Chem. Phys.* **1962**, *36*, 2578.
(9) Maroncelli, M.; Qi, S. P.; Strauss, H. L.; Snyder, R. G. *J. Am. Chem. Soc.* **1982**, *104*, 6237.
(10) Flory, P. J. "Statistical Mechanics of Chain Molecules"; Interscience: New York, 1969.
(11) Jernigan, R. L.; Flory, P. J. *J. Chem. Phys.* **1969**, *50*, 4165.
(12) Yoon, D. Y.; Flory, P. J. *J. Chem. Phys.* **1978**, *69*, 2536.
(13) Wong, P. T. T.; Mantsch, H. H.; Snyder, R. G. *J. Chem. Phys.* **1983**, *79*, 2369.
(14) Flory, P. J.; Vrij, A. *J. Am. Chem. Soc.* **1963**, *85*, 3548.
(15) Eyring, H.; Hirschfelder, J. O. *J. Phys. Chem.* **1937**, *41*, 249.
(16) Prigogine, I. "The Molecular Theory of Solutions"; Interscience: New York, 1957.
(17) Salem, L. *J. Chem. Phys.* **1962**, *37*, 2100.
(18) Gelbart, W. M.; Gelbart, A. *Mol. Phys.* **1977**, *33*, 1387.
(19) Orwoll, R. A.; Flory, P. J. *J. Am. Chem. Soc.* **1967**, *89*, 6814.
(20) Schaerer, A. A.; Busso, C. J.; Smith, A. E.; Skinner, L. B. *J. Am. Chem. Soc.* **1955**, *77*, 2017.
(21) Templin, P. R. *Ind. Eng. Chem.* **1956**, *48*, 154.
(22) Sackmann, H.; Venker, P. *Z. Phys. Chem. (Leipzig)* **1951**, *199*, 100.
(23) Nelson, R. R.; Webb, W.; Dixon, J. A. *J. Chem. Phys.* **1960**, *33*, 1756.
(24) Dollhopf, W.; Grossmann, H. P.; Leute, U. *Colloid Polym. Sci.* **1981**, *259*, 267.
(25) Wurflinger, A. *Faraday Discuss. Chem. Soc.* **1980**, *69*, 146.
(26) Wurflinger, A.; Schneider, G. M. *Ber. Bunsen-ges. Phys. Chem.* **1973**, *77*, 121.
(27) Finke, H. L.; Gross, M. E.; Waddington, G.; Huffman, H. M. *J. Am. Chem. Soc*, **1954**, *76*, 333.
(28) Rossini, F. D.; Pitzer, K. S.; Arnett, R. L.; Braun, R. M.; Pimentel, G. C. "Selected Values of Physical and Thermodynamic Properties of Hydrocarbons and Related Compounds"; Carnegie: Pittsburgh, 1953.
(29) Messerly, J. F.; Guthrie, G. B.; Todd, S. S.; Finke, H. L. *J. Chem. Eng. Data* **1967**, *12*, 338.
(30) Garner, W.; Bibber, K. V.; King, A. M. *J. Chem. Soc.* **1931**, 133, 1533.
(31) Heitz, W.; Wirth, T.; Peters, R.; Strobl, G.; Fischer, E. W. *Makromol. Chem.* **1972**, *162*, 63.
(32) Illers, H. K. *Makromol. Chem.* **1968**, *118*, 88.
(33) Wunderlich, B.; Czornyj, G. *Macromolecules* **1977**, *10*, 906.
(34) Mandelkern, L.; Stack, G. M. *Macromolecules* **1984**, *17*, 871.
(35) Broadhurst, M. G. *J. Res. Natl. Bur. Stand., Sect. A* **1966**, *70A*, 481.
(36) Robertson, R. E. *Macromolecules* **1969**, *2*, 250.

Interaction between Two Adsorbed Polymer Layers

J. M. H. M. Scheutjens* and G. J. Fleer

Laboratory for Physical and Colloid Chemistry, Agricultural University, 6703 BC Wageningen, The Netherlands. *Received July 9, 1984*

ABSTRACT: The effect of adsorbing homopolymer on the interaction between two parallel surfaces is examined in some detail. The results are relevant for the stabilization and flocculation of colloids by adsorbed polymer. The free energy of interaction is derived directly from the partition function using a previously developed lattice model for adsorption of polymers from solution. Comparison with other theories shows partial agreement as well as remarkable discrepancies. Results are presented for a system in full equilibrium with a polymer solution of constant concentration and for a system with a constant amount of polymer between the surfaces. At full equilibrium the force between the surfaces is always attractive due to bridging polymer. With decreasing surface separation a part of the polymer molecules leaves the gap, an increasing fraction of the remaining polymer adsorbs on both surfaces simultaneously, and eventually a monolayer of polymer segments sticks the surfaces together. When the polymer is unable to leave the gap, a strong repulsion between the surfaces appears at small separations and the interaction free energy is mainly determined by the adsorbed amount of polymer, irrespective of chain length. With a large amount of polymer between the surfaces the force is always repulsive, except in a very poor solvent. At smaller surface coverages a minimum in the free energy of interaction develops as a function of surface separation. Recent experimental data confirm our prediction that bridging attraction can also occur in good solvents. As the adsorption of polymer increases with increasing chain length, high molecular weight polymer is a better stabilizer than low molecular weight polymer.

I. Introduction

Polymer adsorption is a very effective tool for controlling the stability of colloidal suspensions.[1-3] For instance, high molecular weight flocculants rapidly remove the last submicroscopic particles in one of the last stages of water treatment. In this case uncovered particles are caught by tails and loops extending from covered ones, so that polymer bridges are formed. The same mechanism is operating in particle separation by flotation.[4,5] Bridging can occur only when the adsorbed amount of polymer is below saturation. At high polymer concentrations all particles are fully covered and the dangling tails and loops form a steric barrier against flocculation. Steric stabilization has important applications in paint industry and food technology. In all these phenomena, steric and/or bridging interactions constitute an important contribution,

0024-9297/85/2218-1882$01.50/0

but in most cases it is not the only one. In addition, van der Waals forces and electrostatic interactions may play a role.

A variety of polymers, including copolymers, polyelectrolytes, and proteins, are applied to obtain the desired effects. In most instances the complexity of these materials, usually commercial products, is such that even the trends cannot be predicted. For monodisperse homopolymers, however, a detailed picture becomes feasible. The interaction between two polymer layers of this type is the result of a subtle balance between entropic repulsion, free energy of mixing, and bridging attraction. To quantify this interaction the segment density distribution of the polymer between two approaching particles, especially in the overlap region, is required. It can be obtained from a suitable polymer adsorption theory. In such a theory several factors have to be taken into account: the interaction of segments and solvent molecules with the surface, that between segments and solvent in the concentrated surface region, and the loss of configurational entropy of the adsorbed polymer chains.

The first theories that incorporate all these effects to a reasonable approximation divide the adsorbed layer into a train layer in contact with the surface and an adjacent loop layer with a predetermined shape of the segment profile, for instance a step function[6] or an exponential decay.[7] For computational convenience the tail fraction was neglected in these theories.

A complete multilayer theory for adsorption of chain molecules from high solution concentrations was developed by Ash et al.[8] and also used for the calculation of interaction forces between parallel plates.[9] Unfortunately, the numerical computations were limited to chains of only four segments per chain. Although currently for most computers a chain length of 10 segments seems tractable with this model, it will be long before the polymer range is reached. Therefore some modifications are necessary in order to obtain results for long chains.

A considerably simpler multilayer theory for all chain lengths was developed by Roe.[10] A crucial step in its derivation is the assumption that the ranking number of a segment in the chain is irrelevant for its spatial distribution. This boils down to density distributions for "loops" and "tails" that are of identical shape, which is more or less equivalent to the neglect of end effects. Therefore, a correct prediction of the segment density beyond the loop region can not be expected when tails are present.

The self-consistent field multilayer theory of Scheutjens and Fleer[11] is more accurate, because this simplifying assumption is avoided. This theory accounts fully for all possible polymer conformations, including those with tails. The generation of the extremely high number of different conformations was possible by adopting the elegant matrix procedure developed by DiMarzio and Rubin.[12,13] Results for almost the whole range of relevant molecular weights can be obtained with this theory. For short molecules the results of Ash et al. are recovered, whereas the densities in the train and loop region agree with the results of Roe. For longer chains, a substantial fraction of the segments are found in tails, which extend far into the solution.

The development of scaling analyses[14,15] might give additional information about adsorbed polymer layers. This technique was first introduced in polymer statistics by de Gennes[16] and employs the analogies between magnetic systems and polymers.

Monte Carlo approaches are still in the state of the single-chain problem.[17,18] For a system of many competing polymer molecules, the introduction of a Flory–Huggins type of mixing energy seems promising for more realistic results.[19]

The structure of an adsorbed polymer layer at finite solution concentrations is now well established[6,7,10,11,20–24] and quite different from the properties of single chains. Below, we give a summary of the most important results.

In dilute and semidilute solutions, the adsorbed amount depends only very weakly on the concentration in the bulk solution; i.e., the adsorption isotherms are of the high-affinity type with a nearly horizontal pseudoplateau. Adsorption from good solvents is low and hardly dependent on molecular weight. In poor solvents, the adsorbed amount increases with increasing chain length. The extension of the polymer layer depends on such parameters as the segmental adsorption energy, the solvent quality, the solution concentration, and the chain length, but it is found that for a given adsorption energy and solvent quality the layer thickness is a function of the adsorbed amount only. In other words, the layer thickness is the same for relatively short chains at high concentrations and for longer chains at (much) lower concentrations, provided the adsorbed amount is the same.[22] Similarly, for a given chain length and solution concentration, the layer thickness is rather insensitive to both adsorption energy and solvent quality. In this case the adsorbed amount increases with increasing adsorption energy or decreasing solvent quality, without affecting the extension of the adsorbed layer, because only the segment densities close to the surface change.[22,23]

When the adsorbed amount is below the pseudoplateau value the polymer lies flat on the surface, forming long trains and short loops. Tails are absent in this case and the solution concentration is extremely low (below an experimentally detectable level). In the pseudoplateau region the fraction of occupied surface sites is essentially independent of the solution concentration and the molecular weight; its magnitude is determined by the adsorption energy and solvent quality. Already at semidilute concentrations the tails protude far into the solution,[22,25,26] determining completely the layer thickness, whereas the loops remain rather small. The train size and the fraction of segments in trains decrease steadily with increasing bulk solution concentration.

For heterodisperse polymers many of the properties given above are different.[27] The reason is that the chains with the highest affinity for the surface (high molecular weight, high adsorption energy) will ultimately displace all other polymer from the surface. Thus, the composition of the adsorbed layer is a function of the available area and the total amount of polymer in the system. Therefore, in order to check theoretical predictions, it is essential to have experimental data for monodisperse polymers. Unfortunately, the availability of such polymer is very poor, and only very few experimental studies are amenable to comparison with theory.

The statistical mechanical treatment of the interaction between two particles covered with polymer was initially restricted to the case of a single chain between parallel plates.[13,28,29] The neglect of lateral interactions led to results which are of very limited validity for the many-chain problem. Mackor and van der Waals[30] introduced separate surface and bulk phases to overcome this problem. They studied the interaction due to terminally adsorbing rigid rods (dimers and tetramers) in equilibrium with a bulk solution and found a repulsive force. The application of self-consistent field theories has improved the models considerably.[9] Most of the results are obtained for grafted polymer, i.e., chains with one or both ends bound to the

surface.[31-36] Unfortunately, in some cases incorrect free energy equations were used, mainly because these theories did not lead to the complete partition function.

Dolan and Edwards[34] obtained the excluded volume parameter which determines the self-consistent field strength, by comparing their free energy equation with the Flory–Huggins equation for the free energy of mixing.[37] They supposed that the free energy is only determined by the change in configurational entropy of the chains. As we will show in the theoretical section, their excluded volume parameter is too small. Apart from that, they neglect higher order terms which become dominant at very high segment densities.

Levine et al.[36] used a model similar to ours to calculate the force between two plates due to grafted polymer. For adsorbing polymer they found qualitatively the same trends as we find. They came to the correct conformational entropy but missed the accompanying correction to the free energy equation of Dolan and Edwards.

For the important case of (nonanchored) homopolymers we must distinguish between *full* thermodynamic equilibrium, when the chains can leave the gap, and *restricted* equilibrium, when for instance during the Brownian collision of two particles the adsorbed polymer is trapped between them. In the latter case the individual segments might still adjust themselves to a local thermodynamic equilibrium, i.e., may adsorb or desorb, whereas the total amount of polymer in the gap remains constant. In such a restricted equilibrium, an exchange between trains, loops, tails, and bridges occurs within the requirement of minimum free energy of the (constant) amount of polymer and the (changing) amount of solvent in the gap, but the chemical potential of the chains in the gap is no longer the same as in the solution.

For adsorbing tetramers in full equlibrium, Ash and Findenegg[9] found attraction between the plates when all segments are of an adsorbing type. If some of the segments are nonadsorbing, repulsion is predicted. de Gennes[38] elaborated an equation for the surface free energy from Cahn[39] to study the interaction due to adsorbed homopolymer. He arrived at the conclusion that the net force is *always attractive* when the polymer may leave the space between the plates. The chains will escape when the plates are approaching each other, so that the segment density in the gap will never increase. The attractive force originates from the bridging effect. When the polymer is not able to escape, the density between the plates will increase with decreasing plate distance and an extra repulsive force results. Using a mean field approximation, de Gennes found a cancellation between volume repulsion and bridging attraction in good solvents. Applying scaling concepts, however, led to the conclusion that the net force is *always repulsive*.

Using the same (mean field) Cahn–de Gennes analysis, Klein and Pincus[40] found the interaction force in poor solvents to be attractive in a distance region comparable with the radius of gyration of the chain in solution and repulsive at shorter plate separations. The attractive force occurs if the concentration between the plates passes the biphasic region of the bulk phase diagram. Experimental work by Klein[41,42] has shown a similar shape of the interaction curve for polystyrene adsorbed on mica sheets.

In the present paper we apply our adsorption model[11,22] to compute the interaction force between parallel plates under different conditions. In the full equilibrium case we find *always attraction*, in agreement with other theories.[9,38] This result differs from that in an earlier paper by us,[43] which contains a serious error.[44] At restricted equilibrium a *minimum in the free energy* is found at low solution concentrations in all solvents. This contradicts de Gennes' mean field result and even more his scaling approach for good solvents,[38] but it is consistent with recent results of Klein and co-workers.[45,46] The attractive force is attributed to an increase of the entropy by bridging. We feel that the Cahn–de Gennes approach underestimates the restrictions imposed by the walls on the conformational entropy of the chains, at least in the one-wall problem. In this analysis, even the sign of the force becomes mainly determined by the solution properties of the polymer.

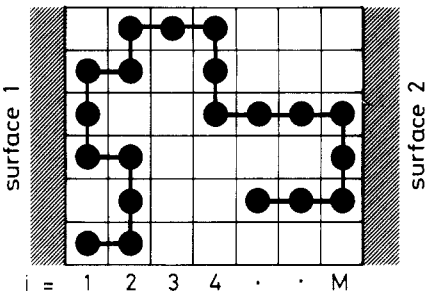

Figure 1. A chain of 20 segments in a lattice between two surfaces. This particular conformation has 4 segments adsorbed on surface 1 and 3 on surface 2. According to eq 12 and 17 the total number of chains in this conformation is $LC\ \lambda_0^9\lambda_1^{10}P_1^4P_2^5P_3^1P_4^3P_5^2P_6^2P_7^3$.

At high concentrations we find always repulsion in good solvents.

We will also apply the theory of Roe[10] and show interaction curves obtained from this model.

II. Theory

A. Model. In deriving the relevant equations, we follow roughly ref 10 and 11. Consider a lattice between two parallel plates. Each lattice site has z neighbors, a fraction λ_0 of which is in the same layer and a fraction λ_1 in each of the adjacent layers. In a simple cubic lattice $z = 6$, $\lambda_0 = {}^4/_6$, and $\lambda_1 = {}^1/_6$. The lattice layers, being parallel to the surface, are numbered $i = 1, 2, ..., M$ and have L lattice sites each. For the sake of generalization, we define a parameter λ_{i-j} such that $z\lambda_{i-j}$ gives the number of immediate neighbors that a site in layer i has in layer j. It is obvious that $\lambda_{i-j} = \lambda_0$ if $i = j$, $\lambda_{i-j} = \lambda_1$ if $i = j \pm 1$, and $\lambda_{i-j} = 0$ otherwise. For a site in layers 1 and M the total number of neighbors is $z\lambda_0 + z\lambda_1 = z(1 - \lambda_1)$. More formally, we can write

$$\sum_{j=1}^{M}\lambda_{i-j} = 1 - \lambda_1\delta_{i,1} - \lambda_1\delta_{i,M} \qquad (1 \le i \le M) \qquad (1)$$

where the Kronecker delta $\delta_{i,j}$ is 1 when $i = j$ and zero otherwise. A lattice site is occupied either by a solvent molecule or a polymer segment. A polymer molecule is represented by a chain of connected segments numbered $s = 1, 2, ..., r$. Segments and solvent molecules in the layers 1 and M are considered to be adsorbed (Figure 1).

The polymer chains and solvent molecules are distributed over the lattice in such a way that the free energy is at its minimum. Since in equilibrium the various conformations of the chains are not equally probable, we must at least distinguish all conformations which differ in energy. The energy of a particular conformation is determined by the number of its adsorbed segments and the interaction with neighboring segments and solvent molecules, which depends on the local concentration. As yet, it is not possible to account for all local fluctuations which may occur. Obviously, the most important fluctuations are expected in the direction normal to the plates. We

neglect the variations within each lattice layer and use an average volume fraction ϕ_i of polymer and a fraction $\phi_i^\circ = 1 - \phi_i$ of solvent in layer i. Let the total number of segments and solvent molecules in layer i be n_i and n_i°, respectively, and the total number of chains between the plates n:

$$\phi_i = n_i/L; \qquad \phi_i^\circ = n_i^\circ/L \tag{2}$$

$$nr + \sum_{i=1}^{M} n_i^\circ = ML \tag{3}$$

Using eq 2 for the local concentration in each layer is equivalent to the well-known mean field or Bragg–Williams approximation; i.e., the distribution within a layer is not affected by mutual interactions. Thus, for the energy of a conformation c it is sufficient to specify the number of segments $r_{i,c}$ that this conformation has in each of the lattice layers. Obviously

$$\sum_c r_{i,c} n_c = n_i \tag{4}$$

$$\sum_{i=1}^{M} r_{i,c} = r \tag{5}$$

where n_c is the number of chains in conformation c.

B. Partition Function. The grand partition function Ξ of the system in equilibrium with a bulk solution is given by a summation of canonical partition functions Q, weighted with the appropriate Boltzmann factors:

$$\Xi = \sum_{\text{all } n_c\text{'s}} Q(\{n_c\},V,A,T) \exp(\mu^\circ \textstyle\sum_i n_i^\circ/kT) \exp(\mu \sum_c n_c/kT) \tag{6}$$

where μ° and μ are the chemical potentials of the solvent molecules and the polymer chains with respect to the reference state, respectively, V is the volume between the plates, A is the area per plate, and T is the temperature. We replace the sum by the maximum term, which is obtained by differentiating ln Ξ with respect to n_d:

$$\left[\frac{\partial \ln Q}{\partial n_d}\right]_{\{n_{c\neq d}\},V,A,T} + (\mu - r\mu^\circ)/kT = 0 \tag{7}$$

The second term of eq 7 follows from the substitution of $\sum n_i^\circ = ML - r\sum n_c$. The physical process corresponding to the differentiation of ln Ξ is transporting one chain from the bulk solution to the gap between the surfaces and placing $r_{i,d}$ segments in each layer i, while the same number of solvent molecules from each layer i is brought to the bulk solution. For $Q(\{n_c\},V,A,T)$ we may write

$$Q = Q_+^\circ Q_+ [\Omega(\{n_c\})/\Omega_+] \exp(\chi_s n_1 + \chi_s n_M) \exp(-\chi \textstyle\sum_i n_i^\circ \langle\phi_i\rangle) \tag{8}$$

where Q_+ is the partition function of n polymer chains in pure polymer liquid and Q_+° the same for n° solvent molecules between two plates of area A each. The first exponental factor accounts for the surface interactions of n_1 and n_M adsorbed segments, displacing n_1 and n_M adsorbed solvent molecules. The adsorption energy of solvent on the plates is included in Q_+°. The difference in adsorption energy is $-\chi_s kT$ per segment–solvent exchange. The second Boltzmann factor contains the energy of mixing the solvent and polymer chains in accordance with the concentration profile. The total number of segment–solvent contacts is $\sum n_i^\circ \langle\phi_i\rangle z$, where $\langle\phi_i\rangle$ is the fraction of contacts with segments for a solvent molecule in layer i. With the Bragg–Williams approximation within each layer, $\langle\phi_i\rangle$ is given by

$$\langle\phi_i\rangle = \lambda_1\phi_{i-1} + \lambda_0\phi_i + \lambda_1\phi_{i+1} = \sum_{j=1}^{M} \lambda_{i-j}\phi_j \tag{9}$$

The Flory–Huggins parameter χ enters because for each solvent molecule which is transferred from pure solvent to a site surrounded by segments ($\langle\phi_i\rangle = 1$) the energy of mixing is χkT.

The combinatory factor $\Omega(\{n_c\})$ in eq 8 gives the number of ways of arranging n polymer molecules and n° solvent molecules in accordance with the conformation profile $\{n_c\}$. It replaces Ω_+, the configurational part of Q_+, representing the number of ways of placing n polymer molecules on rn lattice sites in liquid polymer. Ω_+ has been derived by Flory:[37]

$$\Omega_+ = \left(\frac{z}{rn}\right)^{(r-1)n} \frac{(rn)!}{n!} \tag{10}$$

The factorial $(rn)!$ accounts for the number of ways of placing rn distinguishable monomers; $z/(rn)$ is a correction factor for the $r - 1$ monomers of a chain that are linked to a previously placed monomer and, hence, have only z instead of rn a priori possible locations. Strictly speaking, z represents the effective number of bond directions for each additional segment and decreases somewhat with the number of bonds per chain if a correction is made for the exclusion of conformations with internal overlapping segments. The factorial $n!$ corrects for the indistinguishability of the n chains. Applying a similar equation for the n° solvent molecules ($r = 1$) would give $\Omega_+^\circ = 1$. Hence, a correction for Ω_+° in eq 8 is not necessary.

The combinatory factor Ω has been derived before:[11]

$$\Omega(\{n_c\}) = \left(\frac{z}{L}\right)^{(r-1)n} \prod_c \frac{\omega_c^{n_c}}{n_c!} \prod_i \frac{L!}{n_i^\circ!} \tag{11}$$

There is a close analogy between eq 10 and 11. The M factorials $L!$ give the number of ways of placing $r\sum n_c$ distinguishable monomers and $\sum n_i^\circ$ solvent molecules. The correction factor for the $(r - 1)$ linking segments of a chain in conformation c is $\omega_c(z/L)^{r-1}$, where $\omega_c z^{r-1}$ is the number of arrangements within conformation c when the first segment (or the center of gravity) of the chain is fixed. For instance, when step reversals are allowed, each bond parallel to the surface can point into $\lambda_0 z$ directions and each bond crossing to an adjacent layer has $\lambda_1 z$ choices. Then, if q is the number of bonds in conformation c that are parallel to the surface, we have $(\lambda_0 z)^q(\lambda_1 z)^{r-1-q}$ arrangements within this conformation and ω_c is given by

$$\omega_c = \lambda_0^q \lambda_1^{r-1-q} \tag{12}$$

Note that many arrangements exist with the same segment distribution $\{r_{i,c}\}$, but with a different order of bond directions. According to the current definition, they are grouped into different conformations, because we define a conformation by a specific order of λ_0's and λ_1's.

C. Conformation Probability. The equilibrium distribution of conformations is given by the value of $\{n_c\}$ corresponding to the maximum term in the grand partition function Ξ and is obtained from eq 7 after substitution of eq 8, 10, and 11. The logarithm of $\Omega(\{n_c\})/\Omega_+$ can be approximated by using Stirling's formula:

$$\ln(\Omega/\Omega_+) = ML \ln L - \sum_c n_c \ln(n_c/\omega_c) - \sum_i n_i^\circ \ln n_i^\circ - n \ln r - (r-1)n \ln L \tag{13}$$

While performing the differentation indicated in eq 7, one must realize that $n_i^\circ = L - \sum_c r_{i,c} n_c$ and $\sum n_i^\circ \langle\phi_i\rangle = \sum n_i \langle\phi_i^\circ\rangle$. The result is

$$\ln (n_d/L) = \ln C + \ln \omega_d + \sum_{i=1}^{M} r_{i,d} \ln P_i \qquad (14)$$

where

$$\ln C = r - 1 - \ln r + (\mu - r\mu^\circ)/kT \qquad (15)$$

and

$$\ln P_i = \chi_s(\delta_{1,i} + \delta_{M,i}) + \chi(\langle\phi_i\rangle - \langle\phi_i^\circ\rangle) + \ln \phi_i^\circ \qquad (16)$$

From eq 14 it follows that the number of chains in conformation c is given by

$$n_c/L = C\omega_c \prod_{i=1}^{M} P_i^{r_{i,c}} \qquad (17)$$

Hence, n_c is proportional to a multiple product of weighting factors. According to eq 12, the factor ω_c is a product of $r - 1$ *bond weighting factors* λ_0 (for each "parallel" bond) or λ_1 (for each "perpendicular" bond) and accounts for the relative number of arrangements in conformation c. Each segment in layer i contributes a *segmental weighting factor* P_i, which is a Boltzmann factor accounting for the free energy change when a solvent molecule in layer i is replaced by a single segment. This Boltzmann factor comprises a contribution for the adsorption energy $-\chi_s kT$ when $i = 1$ or $i = M$, a factor for the interaction energy between segments and solvent ($-\chi\langle\phi_i\rangle kT$ for removing the solvent molecule and $\chi\langle\phi_i^\circ\rangle kT$ for inserting the segment), and a factor for the local entropy $-k \ln \phi_i^\circ$ of the solvent molecule (see eq 16).

D. Normalization Constant. The value for the normalization constant C is given in eq 15 and can easily be found if μ and μ° are constant. This is the case when the polymer between the plates is in *full equilibrium* with an infinitely large bulk solution of constant composition. The chemical potentials μ and μ° have been derived by Flory:[37]

$$\mu/kT = 1 - \phi_* - r\phi_*^\circ + \ln \phi_* + r\chi\phi_*^\circ(1 - \phi_*) \qquad (18)$$

$$\mu^\circ/kT = 1 - \phi_*^\circ - \phi_*/r + \ln \phi_*^\circ + \chi\phi_*(1 - \phi_*^\circ) \qquad (19)$$

where ϕ_* and ϕ_*° are the bulk solution volume fractions of polymer and solvent, respectively. Substitution of eq 18 and 19 into eq 15 gives

$$C = \phi_*/rP_*^r \qquad (20)$$

The quantity P_* is the segmental weighting factor in the bulk solution and is given by $P_* = \phi_*^\circ \exp\{\chi(\phi_* - \phi_*^\circ)\}$ (compare eq 16).

In practical situations, it may be impossible for the polymer chains to diffuse out of the gap when the plates are brought closer. It is useful to define a *restricted equilibrium* by the condition that the total amount of polymer between the plates is constant. Then the chemical potential of the polymer changes with varying plate separation. The normalization constant may now be found from the boundary condition $n = \sum_c n_c$. Summation of eq 17 over all conformations gives

$$C = \frac{n}{LP(r)} = \frac{\theta^t}{rP(r)} \qquad (21)$$

where $\theta^t = \sum\phi_i$ is the total amount of polymer between the plates, expressed in equivalent monolayers, and $P(r)$ is the *chain weighting factor*:

$$P(r) = \sum_c \omega_c \prod_{i=1}^{M} P_i^{r_{i,c}} \qquad (22)$$

In restricted equilibrium, the value for C as calculated from eq 21 may be substituted in eq 20 to obtain an implicit equation for the pseudoequilibrium concentration ϕ_*, i.e., the bulk solution concentration that would be in full equilibrium with the polymer between the plates. Clearly, this pseudoequilibrium concentration is now a function of the plate separation M.

E. Free Energy of Interaction. In full equilibrium the free energy of interaction between the plates is determined by the change in the surface free energy $2\gamma A$.[30] From standard thermodynamics we have $2\gamma A = -kT \ln \Xi$. For our system it is more convenient to derive γ from $dF = 2\gamma a\partial L + \mu^\circ\sum\partial n_i^\circ + \mu\sum\partial n_c$, where $a = A/L$ is the area of a surface site, giving $(\partial F/\partial L)_{\{n_c\},M,T} = 2\gamma a + \mu^\circ M$ because $n_i^\circ = L - \sum_c r_{i,c} n_c$. Taking the derivative of $F = -kT \ln Q$ with respect to L gives, after substitution of eq 13 into eq 8 and using eq 19 for μ°:

$$2(\gamma - \gamma^\circ)a/kT = (1 - 1/r)\theta^{exc} + \sum_i \ln (\phi_i^\circ/\phi_*^\circ) + \chi\sum_i(\phi_i\langle\phi_i\rangle - \phi_*^2) \qquad (23)$$

Here, γ° is the surface tension of pure solvent and $\theta^{exc} = \sum(\phi_i - \phi_*)$ the excess amount of polymer between the plates. Equation 23 has been derived before[11] in terms of $\ln (P_i/P_*)$ for adsorption on a single surface, hence, without the factor 2.

The largest term of eq 23 is the second, which is negative if $\phi_i > \phi_*$. Upon expansion of the logarithm, the linear term cancels exactly against the term θ^{exc}. Hence, for $\chi \leq 0$ the right-hand side of eq 23 is negative, as is to be expected for adsorbing polymer. For $\chi > 0$ the last term of eq 23 gives a positive contribution to the quadratic term of the logarithm expansion, but the same conclusion as to the sign of $\gamma - \gamma^\circ$ applies. (Note: for pure bulk polymer, $\phi_i \to 1$ and $\phi_i^\circ \to 0$, $\sum\ln (\phi_i^\circ/\phi_*^\circ)$ is *not* zero.)

In restricted equilibrium the system is open with respect to solvent but not with respect to polymer. In this case the free energy of interaction is given by $F = -kT \ln \Psi$, where $\Psi(\{n_c\},\mu^\circ,V,A,T) = Q(\{n_c\},V,A,T) \exp(\mu^\circ\sum n_i^\circ/kT)$ is the semigrand partition function.

The characteristic function F at constant amount of polymer $\sum n_c$ is found from the characteristic function $2\gamma A$ at constant chemical potential μ (eq 23) via the relation $F = 2\gamma A + \mu\sum n_c = 2\gamma A + (\mu - r\mu^\circ)L\theta^t/r + \mu^\circ L\theta^t$. From eq 15 we have $(\mu - r\mu^\circ)/kT = \ln C - (r - 1) + \ln r$; hence, substitution of eq 21 and 23 gives

$$(F - F^\circ)/LkT = \frac{\theta^t}{r} \ln \frac{\theta^t}{P(r)} + \sum_i \ln \phi_i^\circ + \chi\sum_i \phi_i\langle\phi_i\rangle - \mu^\circ(M - \theta^t)/kT \qquad (24)$$

Here, F° is the free energy of pure solvent between the plates. The term $-\mu^\circ(M - \theta^t)/kT$ is a very small *attractive* term accounting for the osmotic pressure of the solution outside the plates and will be neglected in the calculations in order to avoid the parameter ϕ_*. When necessary, it can be evaluated from eq 19.

III. Comparison with Other Theories

A. Full Equilibrium. Mackor and van der Waals[30] formulated a theory for stiff rods that may be compared with the present model for dimers. Ash et al.[8,9] developed the statistics for flexible oligomers (up to $r = 4$). They excluded conformations with bond angles less than 90°. Both theories account for the fact that one or two of the z contacts per segment are chemical bonds with other segments rather than physical contacts. Their equations reduce to ours for $z \to \infty$. In our model the above-mentioned refinements are not taken into account. It has been shown that these extensions hardly affect the adsorbed amount of oligomers,[11] whereas the complexity of the equations increases considerably.

The theory of Roe[10] has, in principle, only one more simplification than ours: it assumes that all segments have

the same density distribution, independent of their ranking number in the chain. This assumption is valid for monomers, dimers, and two-dimensional chains parallel to the surface. It appears that Roe's equations are identical with ours for $r = 1$, $\lambda_0 = 1$, or $M = 1$, but not for $r = 2$. This discrepancy is due to the lack of inversion symmetry in Roe's model and has been discussed before.[11] However, his equation for the surface tension (eq 36 of ref 10) for one surface is identical with eq 23 (without the factor 2). A proof of this identity is given in Appendix I. Also for multicomponent systems the relation between surface free energy and segment density profiles is identical. In this case eq 23 is generalized to (see Appendix I)

$$2(\gamma - \gamma^\circ)a/kT = \sum_x (1 - 1/r^x)\theta^{x,\text{exc}} + \sum_i \ln (\phi_i^\circ/\phi_*^\circ) + \tfrac{1}{2}\sum_x\sum_y (\chi^{x\circ} + \chi^{y\circ} - \chi^{xy})\sum_i (\phi_i^x\langle\phi_i^y\rangle - \phi_*^x\phi_*^y) \quad (25)$$

where x and y are the component indices. The double summation over x and y extends over all components, including the solvent. Hence, Roe's equations for the surface tension in terms of ϕ_i are identical with our equations, although the segment density profiles and, hence, the numerical values for γ are different.

B. Restricted Equilibrium. Many theories have been developed for interactions in restricted equilibrium. It is possible to make a detailed comparison of our model with the theories of DiMarzio and Rubin,[13] Meier,[31] Hesselink,[32,33] Dolan and Edwards,[34] and Levine et al.[36] The mathematical details are given in Appendix II. Here we mention only the main conclusions.

Our model reduces completely to that of DiMarzio and Rubin[13] for the limiting case of a single chain ($n = 1$) between two plates. This situation is only of theoretical interest and not relevant for practice.

Meier[31] and Hesselink et al.[32,33] split up the free energy in a volume restriction term and an osmotic term. This boils down to the implicit assumption that all weighting factors P_i are equal, which is approximately correct at low concentrations of (terminally attached) nonadsorbing chains ($\chi_s \approx 0$). Under these conditions eq 24 reduces to

$$(F - F^\circ)/LkT \simeq \frac{\theta^t}{r}\ln\left(\frac{\theta^t}{\sum_c \omega_c}\right) - \sum_i \phi_i \ln P_i + \sum_i \ln \phi_i^\circ + \chi\sum_i \phi_i\langle\phi_i\rangle \quad (26)$$

It can be shown (Appendix II) that the first term of the right-hand side corresponds to the volume restriction term and the sum of the last three terms equals, apart from a constant, the osmotic term $(^1/_2 - \chi)\sum\phi_i^2$. Hence, these theories are correct for low concentrations. A similar conclusion has been drawn by Gaylord.[47]

For a comparison with the model of Dolan and Edwards, eq 26 can be written (Appendix II) as $F - F^\circ \simeq -nkT \ln (\sum_c \omega_c \prod_i P_i^{r_{i,c}/2})$ + constants, which is essentially the free energy function used by these authors.[34] Hence, also their free energy function is correct for low concentrations, but their weighting factor $P_i^{1/2} \simeq \exp\{(^1/_2 - \chi)\phi_i\}$ is just the square root of our weighting factor P_i; i.e., their distribution functions are wrong.

The model of Levine et al.[36] is not restricted to low concentrations and uses nearly the same weighting factor (with ϕ_i for $\langle\phi_i\rangle$, except for $i = 1$ and $i = M$) as we found. However, these authors used a free energy function which is qualitatively wrong. In effect, they missed the middle two terms of eq 24. It can be shown (Appendix II) that this is equivalent to an overestimation of the osmotic term in their model by a factor of about 2.

A detailed comparison with the theory of de Gennes[38] is more difficult because of the differences in the underlying assumptions. In this theory, the free energy is written as a sum of local energies which are a function of the local concentration and concentration gradient only. There are three contributions: (i) a term for the adsorption energy, (ii) a term for the energy of a homogeneous system of concentration ϕ_i, and (iii) a positive gradient term $\kappa(\partial\phi_i/\partial i)^2$ which accounts for the spatial variations of the concentration. A crucial assumption is that κ does not depend on the chain length. It can be shown that the choice $\kappa = (24\phi_i)^{-1}$ as used by de Gennes is consistent with the theory of Helfand for infinite chain length, because in this theory each segment of a chain has the same spatial distribution.[48] In our notation this would apply when $P(i,s) = P(i,s-1)$ for most of the segments (see eq 29). However, we have shown that end effects are usually not negligible, except in special cases.[22] Clearly, end effects decrease with decreasing plate distance, so we expect that the gradient method works best when $M < R_g$, where R_g is the radius of gyration of the polymer molecules in solution.

The most important result of de Gennes' method is that in full equilibrium the interaction force $2\partial\gamma/\partial M$ follows the free energy of a homogeneous solution of concentration $\phi_{M/2}$ (the concentration midway between the plates where the gradient is zero) and is always attractive. In restricted equilibrium, the interaction force follows nearly the osmotic pressure of a solution of concentration $\phi_{M/2}$ and, hence, is always repulsive in good solvents. In poor solvents an attractive region occurs when $\phi_{M/2}$ passes the region of biphasic concentrations.[40]

In section VI.C we will compare the predictions of several theories mentioned above with the outcome of our model.

IV. Segment Density Distributions

The conformation profile $\{n_c\}$ is a function of the weighting factors P_i via eq 14 and the weighting factors are a function of the segment density profile $\{\phi_i\} = \{1 - \phi_i^\circ\}$ via eq 16. In turn, the segment density profile is given by $\phi_i = \sum_c r_{i,c} n_c/L$; see eq 4. Thus, the M weighting factors or volume fractions are implicitly given by M simultaneous equations. In a following section we will discuss these equations in more detail.

Alternatively, one may look for a conformation profile $\{n_c\}$ which gives a segment density profile $\{\phi_i\}$ that is consistent with eq 17 for each conformation. In this way, the number of implicit equations is equal to the number of different conformations and, hence, of order $3^{r-1} \approx 10^{r/2}$ per lattice layer. This method has been used by Mackor and van der Waals[30] and Ash et al.,[8] who reduced the number of conformations by forbidding bond angles less than 90°. It will be clear that this method breaks down for chains longer than a few segments. It is much more economical to have only one equation per lattice layer.

In this section we show how to compute the segment density profile from a given set of weighting factors via the generation of all conformations, i.e., via eq 17 and 4.

For monomers ($r = 1$) there is only one "conformation" per layer and the segment density is just $\phi_i = CP_i$, where C is given by either eq 20 or 21. From eq 22 it follows that $P(1) = \sum P_i$ in this case. As the monomer distribution is proportional to $\{P_i\}$ we may call P_i the *free segment probability*.

For symmetric dimers ($r = 2$) the distribution of the first segment is equal to that of the second; i.e., $\phi_i = 2CP(i,2)$. We define $P(i,r)$ as the *end segment probability* of an r-mer in layer i. For monomers we have

$$P(i,1) = P_i \tag{27}$$

The quantity $P(i,r)$ is a subset of the chain probability $P(r)$, since the number of end segments is equal to the number of chains (for convenience we distinguish the first segment from the last segment of a chain):

$$P(r) = \sum_i P(i,r) \tag{28}$$

For dimers there are three different conformations with the second segment in layer i. From eq 17 it follows that their relative probabilities are $P_{i-1}\lambda_1 P_i$, $P_i\lambda_0 P_i$, and $P_{i+1}\lambda_1 P_i$, respectively. Summation gives $P(i,2) = P_i\langle P_i\rangle = P_i\langle P(i,1)\rangle$, where the notation with angular brackets denotes a weighted average over three lattice layers; compare eq 9.

For chains longer than dimers the spatial distribution of the segments is a function of their ranking number in the chain. The distribution of the last segment (and that of the first segment) is given by $CP(i,r)$. To avoid a considerable amount of computing time and complexity, we approximate $P(i,r)$ by assuming that the position of the last segment of a chain is determined by its predecessor and not by the position of other segments; i.e., we generate the chain conformations by a step-weighted random walk adding one segment (s) per step. Thus, $P(i,s)$ follows from the end-segment probabilities $\{P(i,s-1)\}$ of a chain of $s-1$ segments by the recurrent relation

$$P(i,s) = P_i\langle P(i,s-1)\rangle \tag{29}$$

where P_i accounts for the weighting factor of segment s and the angular brackets for the bond weighting factor of the bond between segment s and $s-1$. We note that eq 29 is an alternative representation of the matrix notation developed by DiMarzio and Rubin.[13] Starting from a monomer, for which $P(i,1) = P_i$, the end-segment probabilities of longer chains are calculated by applying eq 29 for each additional segment.

With a step-weighted random walk it is easy to compute the distribution of segment s in a chain or r segments, because the conformations of the first subchain of $s-1$ segments are independent of the positions of the last $r-s$ segments of the chain. Consequently, the total weight of all conformations with segment s in layer i is given by $\langle P(i,s-1)\rangle P_i\langle P(i,r-s)\rangle = P(i,s)P(i,r-s+1)/P_i$. The contribution to the segment density distribution due to all segments s is obtained after normalization

$$\phi_i(s) = CP(i,s)P(i,r-s+1)/P_i \tag{30}$$

Note that segment s has indeed the same distribution as segment $r-s+1$, i.e., $\phi_i(s) = \phi_i(r-s+1)$: the inversion symmetry is obeyed. Summation over all segments gives the overall segment density distribution.

$$\phi_i = C\sum_{s=1}^{r} P(i,s)P(i,r-s+1)/P_i \tag{31}$$

A. Adsorbing, Bridging, and Free Polymer. Once the weighting factors $\{P_i\}$ are known for a given system, it is possible to obtain a very detailed picture of the structure of the polymer between the plates, because the number of chains in each conformation is given by eq 17. We will subdivide the amount of polymer θ^t between the plates into five groups of chains: (i) nonadsorbed chains, θ^f, (ii) chains adsorbed on the first plate only, $\theta^{a'}$, i.e., with segments in layer 1 and none in layer M, (iii) chains adsorbed on the second plate only, $\theta^{a''}$, (iv) bridging chains with the last chain end leaving from the first plate, $\theta^{b'}$, and (v) bridging chains with the last chain end leaving from the second plate, $\theta^{b''}$. Bridging chains have segments in layer 1 as well as in layer M.

If the plates are identical the segment distribution will be symmetric and hence, $\theta^{a'} = \theta^{a''}$ and $\theta^{b'} = \theta^{b''}$. Obviously

$$\sum_G \theta^G = \theta^t \tag{32}$$

where G denotes f, a′, a″, b′, or b″. For each group defined above we can define a chain probability $P^G(r)$ which represents the sum of the weights of all conformations belonging to group G, so that

$$\sum_G P^G(r) = P(r) \tag{33}$$

Normalization of $P^G(r)$ gives the number of chains in group G. Hence, similar to eq 21

$$\theta^G = CrP^G(r) \tag{34}$$

The chain probabilities $P^G(r)$ can be expressed as a sum of end-segment probabilities $P^G(i,r)$ (compare eq 28)

$$P^G(r) = \sum_i P^G(i,r) \tag{35}$$

The generation of end-segment probabilities $P^G(i,s)$ of chains of s segments is straightforward. From eq 29 and the condition that $P(i,s) = \sum_G P^G(i,s)$ it follows that

$$P(i,s) = P_i\langle P^f(i,s-1) + P^{a'}(i,s-1) + P^{a''}(i,s-1) + P^{b'}(i,s-1) + P^{b''}(i,s-1)\rangle \tag{36}$$

The quantity $P^f(i,s)$ is the end-segment probability of all chains, s segments long, ending in layer i and never touching one of the surfaces. From this definition it is easy to see that the term $P_i\langle P^f(i,s-1)\rangle$ in eq 36 gives $P^f(i,s)$, except for $i = 1$ and $i = M$

$$P^f(1,s) = 0$$

$$P^f(i,s) = P_i\langle P^f(i,s-1)\rangle \qquad (1 < i < M) \tag{37}$$

$$P^f(M,s) = 0$$

For $i = 1$ we have $P_1\langle P^f(1,s-1)\rangle = P_1\lambda_1 P^f(2,s-1)$, which is the probability of a chain part ending in layer 1 and with the first $s-1$ segments in the layers $1 < i < M$; i.e., the chain part is adsorbed, with its last segment only, on plate 1 and belongs to $P^{a'}(1,s)$. Similarly, $P_M\langle P^f(M,s-1)\rangle$ contributes to $P^{a''}(M,s)$.

The term $P_i\langle P^{a'}(i,s-1)\rangle$ in eq 36 represents the s-mers of which at least one of the first $s-1$ segments is adsorbed on plate 1 and none of them on the second plate. This is only possible when $M > 1$. The chain belongs to $P^{a'}(i,s)$ when $i < M$. When $i = M$, the chain forms a bridge with the last segment of the bridge (segment s) on the second plate; i.e., $P_M\langle P^{a'}(M,s-1)\rangle$ contributes to $P^{b''}(M,s)$. Thus, we can write

$$P^{a'}(1,s) = P_1\langle P^{a'}(1,s-1) + P^f(1,s-1)\rangle \qquad (M > 1)$$

$$P^{a'}(i,s) = P_i\langle P^{a'}(i,s-1)\rangle \qquad (1 < i < M) \tag{38}$$

$$P^{a'}(M,s) = 0$$

and a similar reasoning applies for the end-segment probabilities of s-mers adsorbed on the second plate only:

$$P^{a''}(1,s) = 0$$

$$P^{a''}(i,s) = P_i\langle P^{a''}(i,s-1)\rangle \qquad (1 < i < M) \tag{39}$$

$$P^{a''}(M,s) = P_M\langle P^{a''}(M,s-1) + P^f(M,s-1)\rangle \qquad (M > 1)$$

The last two terms in eq 36 belong to bridging chains. As defined above, such a chain belongs to $P^{b'}(i,s)$ when the last adsorbed segment (i.e., the adsorbed segment with the highest ranking number) is in layer 1 and to $P^{b''}(i,s)$ otherwise. Obviously, $P^{b'}(M,s) = P^{b''}(1,s) = 0$, except when

$M = 1$. When the last segment (s) is in layer 1 the chain contributes to $P^{b'}(1,s)$; when it is in layer M it contributes to $P_b''(M,s)$. The result is

$$P^{b'}(1,s) = P_1\langle P^{b'}(1,s-1) + P^{b''}(1,s-1) + P^{a''}(1,s-1)\rangle \qquad (M > 1)$$

$$P^{b'}(i,s) = P_i\langle P^{b'}(i,s-1)\rangle \qquad (1 < i < M) \qquad (40)$$

$$P^{b'}(M,s) = 0 \qquad (M > 1)$$

and

$$P^{b''}(1,s) = 0 \qquad (M > 1)$$

$$P^{b''}(i,s) = P_i\langle P^{b''}(i,s-1)\rangle \qquad (1 < i < M) \qquad (41)$$

$$P^{b''}(M,s) = P_M\langle P^{b''}(M,s-1) + P^{b'}(M,s-1) + P^{a'}(M,s-1)\rangle \qquad (M > 1)$$

For $M = 1$ all chains belong to either $P^{b'}(1,s)$ or $P^{b''}(1,s)$.

$$P^{b'}(1,s) = P^{b''}(1,s) = P_1\langle P^{b'}(1,s-1)\rangle \qquad (M = 1) \qquad (42)$$

Most of the starting values $P^G(i,1)$ are zero. The nonzero values are

$$P^{a'}(1,1) = P_1 \qquad (M > 1)$$

$$P^{f}(i,1) = P_i \qquad (1 < i < M)$$

$$P^{a''}(M,1) = P_M \qquad (M > 1)$$

$$P^{b'}(1,1) = P^{b''}(1,1) = \tfrac{1}{2}P_1 \qquad (M = 1) \qquad (43)$$

since a monomer in layer 1 is adsorbed on plate 1, a monomer in layer M is adsorbed on plate 2, and it forms a bridge when $M = 1$. A monomer in one of the layers $1 < i < M$ is not adsorbed and hence contributes to $P^f(i,1)$.

The above equations can be used to calculate the end-segment probabilities $P^G(i,s)$ of the various types of chains by repeatedly extending the chain with one segment, starting from a monomer. The $5M$ values of $P^G(i,2)$ are calculated from the various values of $P^G(i,1)$ as given in eq 43 by applying once each of the equations (37–42). From $P^G(i,2)$ we obtain $P^G(i,3)$, etc. The sum of $P^G(i,r)$ over the five values of G equals $P(i,r)$ as defined in eq 28.

B. Segment Distributions of Loops, Tails, and Bridges. In the previous section we have subdivided the polymer between the plates in adsorbing, bridging, and free chains. The same subdivision was made for the end-segment probabilities $P(i,s)$ of s-mers, giving

$$P(i,s) = P^f(i,s) + P^{a'}(i,s) + P^{a''}(i,s) + P^{b'}(i,s) + P^{b''}(i,s) \qquad (44)$$

where f denotes free chains, a′ and a″ denote chains adsorbed on plate 1 and plate 2, respectively, and b′ and b″ denote bridging chains with the last chain end leaving from plate 1 and plate 2, respectively. Here, we will show a very simple procedure to obtain segment distributions of trains, loops, tails and bridges from these end-segment probabilities.

Substitution of $P(i,s)$ and $P(i,r-s+1)$ from eq 44 into eq 30 and performing the multiplication $\{\sum_G P^G(i,s)\}\cdot\{\sum_G P^G(i,r-s+1)\}$ give 25 terms, which are listed in the second column of Table I, where we have dropped the indices i and s. After multiplication by C/P_i, these terms give the distribution of segment s in a free chain, or in a loop, etc. In the third column of Table I we have indicated for each term to which volume fraction segment s contributes, and the corresponding polymer fraction is shown in the fourth column.

For instance, the first line in Table I represents $P^f(i,s)P^f(i,r-s+1)$ and gives the distribution of segment s when both of the chain parts meeting at segment s are not adsorbed, i.e., when segment s belongs to a free chain. Summation over all segments and normalization gives ϕ_i^f, the volume fraction of free chains in layer i.

$$\phi_i^f = C\sum_{s=1}^{r} P^f(i,s)P^f(i,r-s+1)/P_i \qquad (45)$$

Similarly, the second line in Table I refers to conformations in which the first part of s segments of the chain and the second part of $r-s+1$ segments are adsorbed on plate 1 only; i.e., segment s is part of a loop in a chain adsorbed on plate 1 (when $i > 1$) or part of a train in such a chain (when $i = 1$). For $i = M$ both $P^{a'}(i,s)$ and $P^{a'}(i,r-s+1)$ are zero (see eq 38).

The third line in the table corresponds to the distribution of segment s when it belongs to a tail of a chain adsorbed on plate 1, because segment s forms a link between a chain part which is not adsorbed and one which is adsorbed on plate 1. The first term of line 3 accounts for a tail at the beginning of the chain and the second term for a tail at the end. Lines 4 and 5 account for the chains adsorbed on the second plate and are analogous to lines 2 and 3.

The volume fractions of trains, loops, and tails of chains adsorbed on one surface are found after summation over all segments

$$\phi^{a',tr} = C\sum_{s=1}^{r} P^{a'}(1,s)P^{a'}(1,r-s+1)/P_1 \qquad (46)$$

$$\phi^{a'',tr} = C\sum_{s=1}^{r} P^{a''}(M,s)P^{a''}(M,r-s+1)/P_M \qquad (47)$$

$$\phi_i^{a',l} = C\sum_{s=1}^{r} P^{a'}(i,s)P^{a'}(i,r-s+1)/P_i \qquad (i > 1) \qquad (48)$$

$$\phi_i^{a'',l} = C\sum_{s=1}^{r} P^{a''}(i,s)P^{a''}(i,r-s+1)/P_i \qquad (i < M) \qquad (49)$$

$$\phi_i^{a',t} = 2C\sum_{s=1}^{r} P^{a'}(i,s)P^{f}(i,r-s+1)/P_i \qquad (i > 1) \qquad (50)$$

$$\phi_i^{a'',t} = 2C\sum_{s=1}^{r} P^{a''}(i,s)P^{f}(i,r-s+1)/P_i \qquad (i < M) \qquad (51)$$

Table I
Contribution of Segments in Trains, Loops, Tails, Bridges, and Free Chains to the Segment Density[a]

line	term	s contributes to	chain belongs to
1	P^fP^f	free chains	θ^f
2	$P^{a'}P^{a'}$	trains ($i = 1$) or loops ($i > 1$)	$\theta^{a'}$
3	$P^fP^{a'} + P^{a'}P^f$	tails	
4	$P^{a''}P^{a''}$	trains ($i = M$) or loops ($i < M$)	$\theta^{a''}$
5	$P^fP^{a''} + P^{a''}P^f$	tails	
6	$P^{b'}P^{a'}$	trains ($i = 1$) or loops ($i > 1$)	$\theta^{b'}$
7	$P^{b'}P^f$	tails	
8	$P^{a''}P^{a'} + P^{b''}P^{a'}$	bridges	
9	$P^{b''}P^{a''}$	trains ($i = M$) or loops ($i < M$)	$\theta^{b''}$
10	$P^{b''}P^f$	tails	
11	$P^{a'}P^{a''} + P^{b'}P^{a''}$	bridges	
12	$P^{a'}P^{b'} + P^{b'}P^{b'}$	trains ($i = 1$) or loops ($i > 1$)	$\theta^{b'} + \theta^{b''}$
13	$P^{a''}P^{b''} + P^{b''}P^{b''}$	trains ($i = M$) or loops ($i < M$)	
14	$P^fP^{b'}$	tails attached to plate 1	
15	$P^fP^{b''}$	tails attached to plate 2	
16	$P^{b'}P^{b''} + P^{b''}P^{b'} + P^{a'}P^{b''} + P^{a''}P^{b'}$	bridges	
$\sum$	PP	ϕ	θ^t

[a] For explanation, see text.

where the indices tr, l, and t indicate trains, loops, and tails, respectively.

Lines 6–16 in Table I contain 18 terms corresponding to bridging chains. Eight of them (lines 8, 11, and 16) contain two chain probabilities P^a or P^b referring to the two different plates and give the volume fraction ϕ_i^{br} of bridges. Because of the chain symmetry, these can be combined in four terms:

$$\phi_i^{br} = 2C\sum_{s=1}^{r}\{P^{a'}(i,s) + P^{b'}(i,s)\} \times \{P^{a''}(i,r-s+1) + P^{b''}(i,r-s+1)\}/P_i \quad (52)$$

The sum between the first pair of braces in eq 52 represents the first part of the chain connecting segment s with plate 1, and the second sum the other chain part which somewhere meets the second plate.

Of the remaining ten terms in Table I, six contain a product of P^a and P^b referring to the same plate; they represent trains (for $i = 1$ or M) or loops (for $1 < i < M$) of bridging chains (lines 6, 9, 12, and 13). The last four terms (lines 7, 10, 14, and 15) are of the type P^bP^f and correspond to tails belonging to bridging chains. Following a similar reasoning as applied above, the volume fractions of trains, loops, and tails of bridging chains can be written as

$$\phi_i^{b',tr} = C\sum_{s=1}^{r}P^{b'}(1,s)\{2P^{a'}(1,r-s+1) + P^{b'}(1,r-s+1)\}/P_1 \quad (53)$$

$$\phi_i^{b'',tr} = C\sum_{s=1}^{r}P^{b''}(M,s)\{2P^{a''}(M,r-s+1) + P^{b''}(M,r-s+1)\}/P_M \quad (54)$$

$$\phi_i^{b',l} = C\sum_{s=1}^{r}P^{b'}(i,s) \times \{2P^{a'}(i,r-s+1) + P^{b'}(i,r-s+1)\}/P_i \qquad (i > 1) \quad (55)$$

$$\phi_i^{b'',l} = C\sum_{s=1}^{r}P^{b''}(i,s) \times \{2P^{a''}(i,r-s+1) + P^{b''}(i,r-s+1)\}/P_i \qquad (i < M) \quad (56)$$

$$\phi_i^{b',t} = 2C\sum_{s=1}^{r}P^{b'}(i,s)P^{f}(i,r-s+1)/P_i \quad (57)$$

$$\phi_i^{b'',t} = 2C\sum_{s=1}^{r}P^{b''}(i,s)P^{f}(i,r-s+1)/P_i \quad (58)$$

In this way, the segment distributions of trains, loops, tails, and bridges are obtained from the end-segment probabilities derived in the previous section.

C. Train, Loop, Tail, and Bridge Size Distributions. The end-segment probabilities $P^G(i,s)$ contain much more information than we have used above. Of special interest are the numbers and lengths of trains, loops, tails, and bridges in a given system. These quantities can be obtained from $P^G(i,s)$ in different ways, but we will give only the simplest expressions here.

Let us start with the nonbridging chains. Obviously, the expressions for these chains will not differ from those of the one plate model.[22] Hence, the average number of loops, $n^{a',l}$, per chain adsorbed on plate 1, is obtained by following the chain from the first adsorbed segment and counting the number of bonds from layer 2 to layer 1. The total number of such bonds between segment s and segment $s + 1$ is $CP^{a'}(2,s)\lambda_1P^{a'}(1,r-s)$. Since the number of adsorbed chains on the first plate is $CP^{a'}(r)$, we have

$$n^{a',l} = \frac{\lambda_1}{P^{a'}(r)}\sum_{s=2}^{r-1}P^{a'}(2,s)P^{a'}(1,r-s) \quad (59)$$

and similarly

$$n^{a'',l} = \frac{\lambda_1}{P^{a''}(r)}\sum_{s=2}^{r-1}P^{a''}(M-1,s)P^{a''}(M,r-s) \quad (60)$$

The summation starts from $s = 2$, because the smallest possible loop is one segment long, and ends at $s = r - 1$, since the longest possible loop has $r - 2$ segments. As each end of a loop is connected to a train, the number of trains, n^{tr}, per adsorbed chain is given by

$$n^{a',tr} = n^{a',l} + 1; \qquad n^{a'',tr} = n^{a'',l} + 1 \quad (61)$$

Finally, the number of tails, n^t, equals the number of chain ends ($s = r$) not ending on the plate.

$$n^{a',t} = 2 - 2P^{a'}(1,r)/P^{a'}(r); \quad n^{a'',t} = 2 - 2P^{a''}(M,r)/P^{a''}(r) \quad (62)$$

We now examine bridging chains. Their number is $C\{P^{b'}(r) + P^{b''}(r)\}$ and they form not only bridges but also trains on both of the plates and, if the chains are long enough, loops and tails as well.

Following the backbone of each chain, we obtain just half the total number of bridges by counting each entry of layer 1 of a chain part that has a previous segment in layer M. That chain part, consisting of s segments, belongs either to the group $P^{a''}$ (no previous segment in layer 1) or $P^{b''}$ (having a previous bridge). The other chain part of $r - s$ segments is either adsorbed on plate 1 only ($P^{a'}$) or forms another bridge ($P^{b'}$). Analogously to eq 59 we obtain the average number n^b of bridges per chain after summation and normalization:

$$n^b = \frac{2\lambda_1}{P^{b'}(r) + P^{b''}(r)}\sum_{s=M-1}^{r-1}\{P^{a''}(2,s) + P^{b''}(2,s)\} \times \{P^{a'}(1,r-s) + P^{b'}(1,r-s)\} \quad (63)$$

The number of loops on the first plate, $n^{b',l}$, of bridging chains consists of three contributions. The first bond in such a loop connects two subchains, each coming from the first plate, of which (i) only the first subchain is a bridging chain, (ii) only the second subchain is a bridging chain, or (iii) both subchains are bridging chains. The corresponding number of loops ending at s is $CP^{b'}(2,s)\lambda_1P^{a'}(1,r-s)$, $CP^{a'}(2,s)\lambda_1P^{b'}(1,r-s)$, and $CP^{b'}(2,s)\lambda_1P^{b'}(1,r-s)$, respectively. From symmetry it follows that the sum of contribution (i) over s equals the sum of (ii). Hence, the result is

$$n^{b',l} = \frac{\lambda_1}{P^{b'}(r) + P^{b''}(r)}\sum_{s=M+1}^{r-1}P^{b'}(2,s)\{2P^{a'}(1,r-s) + P^{b'}(1,r-s)\} \quad (64)$$

and equivalently

$$n^{b'',l} = \frac{\lambda_1}{P^{b'}(r) + P^{b''}(r)}\sum_{s=M+1}^{r-1}P^{b''}(M-1,s) \times \{2P^{a''}(M,r-s) + P^{b''}(M,r-s)\} \quad (65)$$

The number of trains on plate 1, $n^{b',tr}$, per bridging chain is most easily found by counting the number of train ends. This number is determined by the number of loops (two train ends per loop) and the number of bridges (one train end on each surface per bridge). In addition, each chain end corresponds to one train end. The number of chain ends with the last adsorbed segment on plate 1 and belonging to bridging chains is $2CP^{b'}(r)$. Since the number

of train ends is twice the number of trains, we find for the last number

$$n^{b',tr} = n^{b',l} + \tfrac{1}{2}n^{b} + \frac{P^{b'}(r)}{P^{b'}(r) + P^{b''}(r)} \quad (66)$$

and

$$n^{b'',tr} = n^{b'',l} + \tfrac{1}{2}n^{b} + \frac{P^{b''}(r)}{P^{b'}(r) + P^{b''}(r)} \quad (67)$$

The number of tails equals the number of chain ends minus those which are adsorbed (see also eq 62). The number of chain ends on plate 1 of bridging chains is $2CP^{b'}(r)$, of which $2CP^{b'}(1,r)$ are adsorbed. Consequently, the number of tails on plate 1, $n^{b',t}$, per bridging chain is

$$n^{b',t} = 2\frac{P^{b'}(r) - P^{b'}(1,r)}{P^{b'}(r) + P^{b''}(r)} \quad (68)$$

and similarly

$$n^{b'',t} = 2\frac{P^{b''}(r) - P^{b''}(M,r)}{P^{b'}(r) + P^{b''}(r)} \quad (69)$$

The average fraction of segments, ν, in trains, loops, tails, and bridges can be found from

$$\nu^{G,S} = \sum_{i=1}^{M} \phi_i^{G,S}/\theta^{G} \quad (70)$$

where G (=a', a'', b) refers to one of the chain fractions (adsorbed on plate 1, adsorbed on plate 2, or bridging chains) and S (=tr, l, t, b) denotes trains, loops, tails, or bridges. For example, the fraction $\nu^{a',l}$ of segments in loops of chains adsorbed on plate 1 is the ratio between the sum of all volume fractions $\phi_i^{a',l}$ of loops in these chains and the amount of polymer adsorbed on plate 1.

The average length of such a loop, $l^{a',l}$, is the ratio between the number of segments per chain in these loops, $r\nu^{a',l}$, and the number of loops per chain, $n^{a',l}$. Generally, the length $l^{G,S}$ of a chain part S of the chain fraction G is given by

$$l^{G,S} = r\nu^{G,S}/n^{G,S} \quad (71)$$

It is also possible to obtain the size distributions of trains, loops, tails, and bridges, i.e., the number of chain parts of length s. For example, the number of tails of length s per chains adsorbed on plate 1 is given by[22]

$$n^{a',t}(s) = \frac{2\lambda_1}{P^{a'}(r)} P^{f}(2,s)P^{a'}(1,r-s) \quad (72)$$

whereas the train size distribution of the same polymer fraction is

$$n^{a',tr}(s) = \frac{\lambda_1^{2}\lambda_0^{s-1}P_1^{s}}{P^{a'}(r)} \sum_{t=0}^{r-s} \{P^{a'}(2,t) + P^{f}(2,t)\} \times \{P^{a'}(2,r-s-t) + P^{f}(2,r-s-t)\} \quad (73)$$

For loop and bridge size distributions, the generation of other end-segment probabilities is necessary. The procedures are equivalent to those given in ref 22 and the reader is referred to that paper for more details. An obvious check for the correctness of these equations is the (numerical) check of $n^{G,S} = \sum_s n^{G,S}(s)$.

V. Method of Computation

The M segmental weighting factors $\{P_i\}$ are obtained by solving numerically a set of M simultaneous equations. The values of P_i must be positive. It is therefore convenient to use the unconstrained variables $\{X_i\}$ defined by

$$X_i = \ln P_i \qquad (1 \le i \le M) \quad (74)$$

Starting with $X_i = 0$ $(1 \le i \le M)$, we solve iteratively the following set of equations:

$$P(i,1) = P_i = e^{X_i} \qquad (1 \le i \le M) \quad (27a)$$

$$P(i,s) = P_i\langle P(i,s-1)\rangle \qquad (1 \le i \le M; \quad 2 \le s \le r) \quad (29)$$

$$\phi_i = C\sum_{s=1}^{r} P(i,s)P(i,r-s+1)/P_i \qquad (1 \le i \le M) \quad (31)$$

where $C = \phi_*/(rP_*^{r})$ (full equilibrium) or $C = \theta^{t}/\{r\sum_{i=1}^{M}P(i,r)\}$ (restricted equilibrium)

$$\phi_i^{\circ} = P_i e^{-\chi_s(\delta_{1,i}+\delta_{M,i})-\chi\langle 2\phi_i-1\rangle} \qquad (1 \le i \le M) \quad (16a)$$

until $\phi_i + \phi_i^{\circ} = 1$ (or $\ln(\phi_i + \phi_i^{\circ}) = 0$). In principle, several standard routines solving $f(\{X_i\}) = 0$ are available. For example, a Fortran listing of a powerful routine is given in ref 49.

An important reduction of computer time is possible by further exploiting the symmetry of the equations. For instance, segment s and segment $r - s + 1$ have the same distribution, so whenever G = G' we may replace

$$P^{G}(i,s)P^{G'}(i,r-s+1) \text{ by } P^{G'}(i,s)\,P^{G}(i,r-s+1)$$

or

$$\sum_{s=1}^{r} P^{G}(i,s)P^{G}(i,r-s+1) = \delta(r) + 2\sum_{s=1}^{r-s} P^{G}(i,r-s+1) \quad (75)$$

where $\delta(r) = \{P^{G}(i,{}^1/_2 + r/2)\}^2$ if r is odd and $\delta(r) = 0$ otherwise. This reduces the number of terms by 50%.

In many cases the two surfaces are of the same type, giving a symmetric segment density profile. Then many of the variables are mirror images of each other, for example, $P^{a'}(i,s) = P^{a''}(M-i+1,s)$, $P^{b'}(i,s) = P^{b''}(M-i+1,s)$, $\phi_i^{a'} = \phi_{M-i+1}^{a''}$, $P_i = P_{M-i+1}$, and $X_i = X_{M-i+1}$. The number of simultaneous equations and the number of variables $\{X_i\}$ is thus reduced to $M/2$.

Results given in the following section are obtained by a special program written in Simula67 using a DEC10 computer.

VI. Results and Discussion

In this section a typical collection of the results for a hexagonal lattice ($\lambda_0 = 6/12$) will be shown. Occasionally, data for other lattice types will be mentioned. The effect of molecular weight, adsorption energy, solvent quality, solution concentration, and adsorbed amount on the interaction free energy will be examined in some detail.

The adsorbed amount of polymer is a function of molecular weight, adsorption energy, solvent quality, and solution concentration. The same adsorbed amount can be obtained for different combinations of these quantities. The properties of adsorbed layers at constant solution concentration are qualitatively different from those at constant amount of adsorbed polymer. For instance, at constant solution concentration the root-mean-square thickness of the adsorbed polymer layer on a single surface is nearly independent of both the adsorption energy and the solvent quality and proportional to the square root of the molecular weight of the polymer. On the other hand, at constant adsorbed amount the thickness of the polymer layer decreases with increasing adsorption energy and decreasing solvent power and is independent of the chain length.[22]

For the two-plate problem, the two cases of constant solution concentration and constant amount of polymer represent important extremes. At full equilibrium, the amount of polymer between the plates adapts itself to a

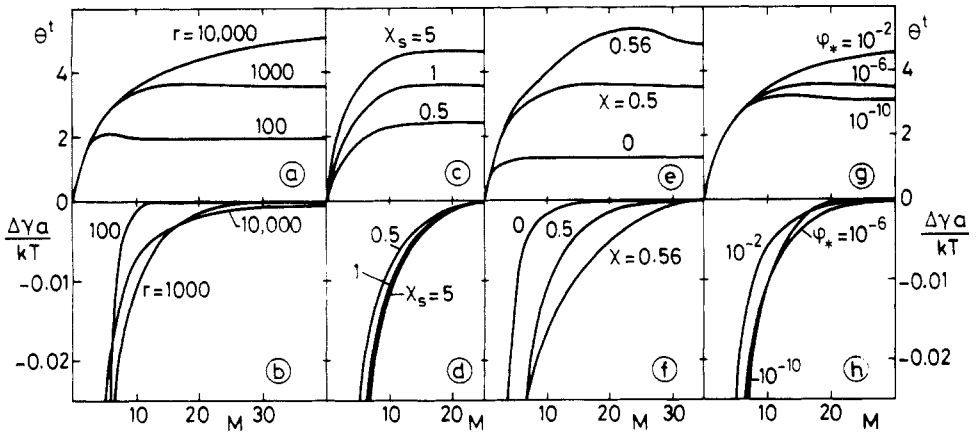

Figure 2. Adsorption and interaction curves at full equilibrium. The top plots show the total amount of polymer between the plates (in equivalent monolayers), and the bottom plots the free energy of interaction (in units of kT per surface site), both as a function of the plate separation M (in lattice layers). In each graph the curve for $\lambda_0 = 0.5$, $\chi = 0.5$, $\chi_s = 1$, $r = 1000$, and $\phi_* = 10^{-6}$ is given together with two curves for which one parameter has either a lower or a higher value, respectively. The effect of chain length is shown in a and b, that of the adsorption energy in c and d, that of the solvent quality in e and f, and the influence of the solution concentration in g and h.

constant solution concentration, whereas at restricted equilibrium the polymer cannot escape from the gap between the plates and the amount of polymer is constant. The former situation is relevant for nonadsorbing polymer or, possibly, when the surfaces are flexible (allowing for lateral compression or diffusion) as is the case for liquid films and liquid–liquid interfaces. A constant amount of polymer is more probable when two polymer covered solid surfaces approach each other. Obviously, in all cases the interaction will be zero at large distances. Also, in restricted equilibrium the free energy of the system will never be lower than that at full equilibrium. Hence, at a given plate separation, the free energy of interaction between two surfaces with a constant amount of polymer between them will be higher than that at full equilibrium, whenever this amount deviates (positively or negatively) from its equilibrium value. However, as we will show below, this deviation is only substantial at small distances. At plate separations corresponding to the minimum in the interaction free energy in restricted equilibrium, the interaction is almost identical with that in full equilibrium. Therefore, we first discuss the equilibrium forces.

A. Full Equilibrium. When the polymer is in equilibrium with a constant bulk solution concentration the interaction between the plates is always found to be attractive. This result supports the analysis of de Gennes.[38] At full equilibrium the interaction free energy is equal to the difference $\Delta\gamma$ between the sum of the two surface free energies $\gamma' + \gamma''$ of the two surfaces at plate separation M and that at infinite separation ($M \rightarrow \infty$). In Figure 2 the total amount of polymer between the plates θ^t (in equivalent monolayers) and $\Delta\gamma$ in units of kT per surface site of one plate) are plotted as a function of the plate separation M (in units of lattice layers) under various conditions. Unless indicated otherwise, the parameters are $\lambda_0 = 0.5$, $\chi = 0.5$, $\chi_s = 1$, $r = 1000$, and $\phi_* = 10^{-6}$.

All interaction curves in Figure 2 are indeed monotonically decreasing with decreasing M, whereas the adsorbed amount of polymer in most cases passes through a (sometimes weak) maximum and decreases at smaller M until all the chains are squeezed out. We discuss the origin of the maximum in θ^t in connection with Figure 4 below. However, the volume fraction of adsorbed segments (trains, not shown in Figure 2) is nearly constant up to very small M and even increases slightly going from $M = 2$ to $M = 1$. Therefore, it is unlikely that the last monolayer of polymer will leave the gap. The ultimate equilibrium situation, having the lowest free energy, will be a sandwich structure of two plates with one layer of polymer segments in between, the concentration of which depends mainly on χ_s and χ.

In parts a and b of Figure 2 the effect of the chain length r is shown. The onset of interaction occurs at a separation comparable to the diameter of a free coil in solution ($\simeq r^{1/2}$) and is determined by the extension of the tails.[22] Consequently, at large distances the free energy of interaction is more negative for longer chains. When the plates come closer, the tails form bridges and the segment density distribution becomes of the loop–bridge type, which is, for small separations, independent of r. The free energy of interaction does not become independent of the chain length, since the free energy of the reference state (γ at $M \rightarrow \infty$) depends on chain length. Because $\gamma(\infty)$ decreases with increasing r, $\Delta\gamma$ at small M becomes more negative for short chains.

The adsorption energy χ_s affects the adsorbed amount of polymer (and hence θ^t; see Figure 2c), without changing the thickness of the adsorbed polymer layer very much.[23] Consequently, the only effect of χ_s on the interaction curves is a small change in magnitude (see Figure 2d). At $\chi_s = 5$ the surfaces are almost fully covered by polymer segments ($\phi_1 = \phi_M \approx 0.995$).

In parts e and f of Figure 2 the effect of the solvent quality is illustrated. In a good solvent (e.g., $\chi = 0$) the adsorption is low, resulting in a relatively short-range interaction and the maximum in the adsorbed amount is either weak or absent. In worse than Θ-solvents ($\chi > 0.5$) the adsorption and the range of interaction increase very rapidly with χ and the adsorption maximum is more pronounced. We will return to this point below.

A last parameter which may be important is the solution concentration (Figure 2g,h). Polymer adsorption isotherms, having a nearly horizontal pseudoplateau, are of the high-affinity type, implying only a weak dependence of the adsorbed amount on the solution concentration. With increasing ϕ_* the change in the number of train segments is much smaller than that in loops and tails. Hence, at large plate separations the interaction is stronger in more concentrated solutions due to more and longer loops and tails. At smaller plate separations the opposite effect occurs because of a different reference state: $\gamma(\infty)$ is smaller in more concentrated solutions.

The main conclusion from Figure 2 is that at full equilibrium both the adsorption energy and the solution

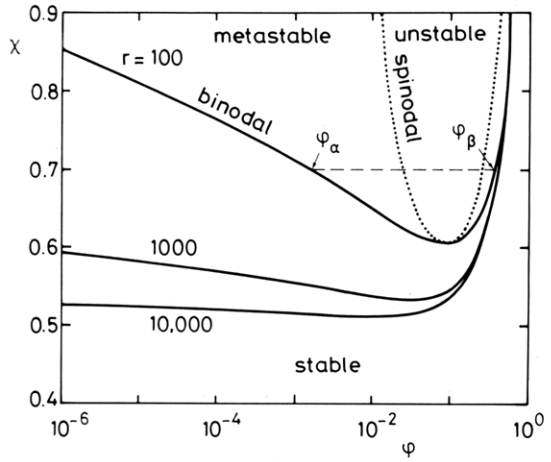

Figure 3. Binodals (full curves) for different chain lengths and the spinodal for $r = 100$ (dotted curve). A binodal gives the boundary between stable and metastable regions, whereas a spinodal indicates the transition between metastable and instable regions. Binodal and spinodal touch at their minimum (critical point). After phase separation, the concentrations of polymer in the two coexisting phases are given by the binodal, e.g., ϕ_α and ϕ_β.

concentration do not affect the interaction substantially. The range of interaction is mainly determined by the chain length and the solvent quality.

We now examine in more detail the forces in poor solvents. In Figure 3 binodal curves, giving the boundary between stable and metastable (bulk) solutions, are shown for three different chain lengths.[37] The minimum of each curve is the critical point, corresponding to $\chi_{cr} = {}^1/_2(1 + r^{-1/2})^2$ and $\phi_{cr} = (1 + r^{1/2})^{-1}$. At any χ above the critical point, there is an unstable region between the two critical compositions of the solution, given by the spinodal (dotted curve for $r = 100$), and two metastable regions between the spinodal and the binodal. The chemical potentials of polymer and solvent (eq 18 and 19) at the lower binodal concentration ϕ_α are equal to those at the higher binodal concentration ϕ_β; i.e., $\mu(\phi_\alpha) = \mu(\phi_\beta)$ and $\mu^\circ(\phi_\alpha^\circ) = \mu^\circ(\phi_\beta^\circ)$. These two equations in two unknowns ($\phi_\alpha = 1 - \phi_\alpha^\circ$ and $\phi_\beta = 1 - \phi_\beta^\circ$) are implicit but can be solved numerically. The spinodal is given by the condition $\delta\mu/\delta\phi = 0$. The free energy of a solution of metastable composition is lower after phase separation in two phases with concentrations ϕ_α and ϕ_β, respectively.

For solution concentrations corresponding to the lower stable region ($\phi_* < \phi_\alpha$) the adsorbed polymer layers are of finite size, although they become thicker when the solution concentration is increased or the solvent quality is decreased (higher χ). Here, we will examine the region near the binodal by changing ϕ_* at constant χ, since ϕ_* is less critical than χ. We choose $r = 100$ and $\chi = 0.7$, giving binodal concentrations of $\phi_\alpha = 0.001\,501\,4$ and $\phi_\beta = 0.371\,36$, respectively. In Figure 4 the adsorption and interaction curves are given for several concentrations of polymer in the bulk solution.

At low concentrations the shapes of the curves are as shown before (compare $\chi = 0.56$ in Figure 2e,f and $\phi_* = 10^{-4}$ in Figure 4a,b). At $\phi_* = 10^{-4}$ the amount θ^t of polymer between the plates consists almost completely of bridging (θ^b) and adsorbing ($\theta^{a'} + \theta^{a''}$) chains; see the dashed curves in Figure 4a. The amount of free chains (θ^f) is negligible. The onset of interaction (Figure 4b) is just at the distance ($M = 15$) where bridges start to appear. The increase of bridging chains pushes the concentration of segments midway between the plates beyond the critical volume fraction of polymer, but the composition between the

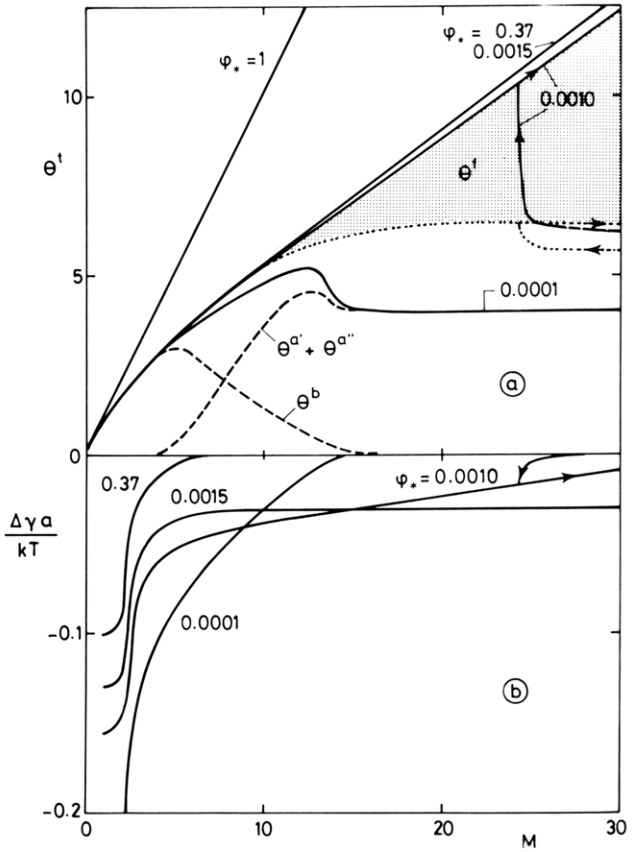

Figure 4. Adsorption (a) and interaction (b) curves at full equilibrium in a poor solvent for different volume fractions of polymer in the solution ($\lambda_0 = 0.5$, $\chi = 0.7$, $\chi_s = 1$, $r = 100$). The binodal concentrations are $\phi_\alpha = 0.001\,501\,4$ and $\phi_\beta = 0.371\,36$, respectively. The curves for $\phi_* = \phi_\alpha$ and $\phi_* = \phi_\beta$ are essentially identical. For concentrations slightly below ϕ_α a hysteresis effect occurs. For $\phi_* = 10^{-4}$ the amount of bridging polymer, θ^b, and the rest of adsorbing polymer, $\theta^{a'} + \theta^{a''}$, are indicated (dashed curves). For $\phi_* = 10^{-3}$ the total amount of adsorbed polymer, $\theta^b + \theta^{a'} + \theta^{a''}$, is shown (dotted curve); the hatched area corresponds to the amount of nonadsorbed polymer, θ^f, at $\phi_* = 10^{-3}$.

plates is not unstable, since the conformational entropy of the chains between the plates is less than that in the bulk solution. The spinodal and binodal curves given in Figure 3 apply only for solutions which are homogeneous over distances of several molecular diameters. However, the higher concentration midway between the plates in combination with a high χ value increases the segmental weighting factors P_i (eq 16) in the loop regions of the adsorbed chains, so that the adsorbed amounts $\theta^{a'}$ and $\theta^{a''}$ increase as well. This effect is smaller at lower solution concentrations, where the bridges appear at shorter distances.

In good solvents ($\chi = 0$), $\theta^{a'}$ and $\theta^{a''}$ decrease when bridges appear but not always enough to compensate the increase in θ^b, e.g., at low concentrations. Hence, also in good solvents a maximum in the adsorption curves due to bridging chains may occur (not shown).

At concentrations close to the binodal, a linear part in the adsorption curve appears with a slope which is equal to the volume fraction $\phi_{M/2}$ midway between the plates. This volume fraction is in the metastable region between the higher spinodal and binodal concentrations, in this case between 0.266 and 0.371. For instance in Figure 4a, the adsorption for $\phi_* = 10^{-3}$ increases linearly from $M = 8$ with a slope 0.36. This increase of θ^t is mainly due to the fraction θ^f (indicated by the shaded area in Figure 4a) of nonadsorbed polymer which fills up the segment density

of loops and tails midway the plates to a nearly constant value of 0.36. The interaction curve is also linear beyond $M = 8$ with a slope that is a measure for the energy of transfer of solvent and polymer from the bulk solution to the space between the surfaces, where the composition is different.

At large plate separations the overlap of adsorbed polymer layers is too small to attract much free polymer and θ^t may suddenly drop to a lower level, so that the concentration $\phi_{M/2}$ becomes equal to ϕ_* and the interaction between the plates jumps to zero. Thus, beyond $M = 24$, there are two equilibrium states, of which the one with the highest free energy is metastable, and a hysteresis between these states occurs when the interplate distance is successively increased and decreased. This process is very similar to condensation and evaporation in pores.

Very close to the binodal concentration, at $\phi_* = 0.0015$, the linear part of the θ^t curve has a slope of 0.37 ($\phi_{M/2} = 0.37$, the upper binodal concentration) and the interaction curve is nearly horizontal. In this case there is essentially no difference between the two coexisting phases in a biphasic system and the solutions inside and outside the gap, respectively.

Obviously, the distance at which the jump occurs goes to infinity for a concentration on the binodal, because that concentration would be in full equilibrium with the higher concentration (also on the binodal) between the plates. Also, there would be no difference in the chemical potentials and hence, in the segment density between the plates, if also the solution concentration were at the higher binodal concentration. The only difference would be a shift in the free energy reference point, γ at $M \rightarrow \infty$. Thus, the adsorption curves for $\phi_* = 0.0015$ and $\phi_* = 0.37$ in Figure 4a coincide, while the two corresponding interaction curves in Figure 4b are identical except for a vertical shift. When $\phi_* \geq 0.37$ and $M \gtrsim 15$ the volume fraction of polymer midway between the plates is close to ϕ_* and the interaction free energy is essentially zero.

B. Restricted Equilibrium. When the polymer is unable to escape from the space between the plates during the approach of the surfaces (θ^t = constant), the chemical potential of the polymer will depend on the interplate distance; i.e., the polymer would be in equilibrium with a bulk solution of continuously changing composition. Hence, the resulting interaction curve is a complicated crossover between many equilibrium curves which, in addition, are to be shifted to the same reference point. However, it is easy to predict some trends. At large distances the interaction between the surfaces will be zero, whereas at a distance $M = \theta^t$, i.e., no solvent between the plates, the repulsion becomes infinite. As stated before, the free energy of interaction of approaching surfaces will be higher whenever the adsorbed amount deviates from its equilibrium value. This is illustrated in Figure 5.

In Figure 5b the interaction curves $\Delta\gamma$ (equilibrium) and ΔF (constant θ^t) are plotted, using the curve for $\phi_* = 10^{-4}$ from Figure 4 for $\Delta\gamma$. At large separations the equilibrium adsorption is such that $\theta^t \approx 4$ (see Figure 5a), so we used $\theta^t = 4$ for the restricted equilibrium curve to obtain the same reference free energy. Since the full equilibrium curve shows a maximum in θ^t, there is another point (at $M \approx 7$) where θ^t is the same for full and restricted equilibrium. At that point restricted and equilibrium gives necessarily the same results as full equilibrium. In Figure 5b we see that this point is very close to the position of the free energy minimum at constant θ^t. At all other distances the nonequilibrium curve is above the equilibrium curve.

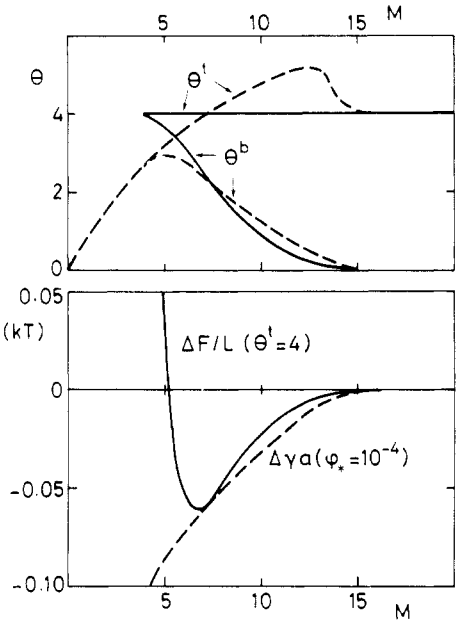

Figure 5. Comparison between adsorption and interaction curves at full equilibrium (dashed curves) and those at constant amount of polymer between the surfaces (full curves). The amount of polymer between the plates at large separation is the same in both cases ($\theta^t = 4$ monolayers), corresponding to $\phi_* = 10^{-4}$. $\lambda_0 = 0.5$, $\chi = 0.7$, $\chi_s = 1$, and $r = 100$.

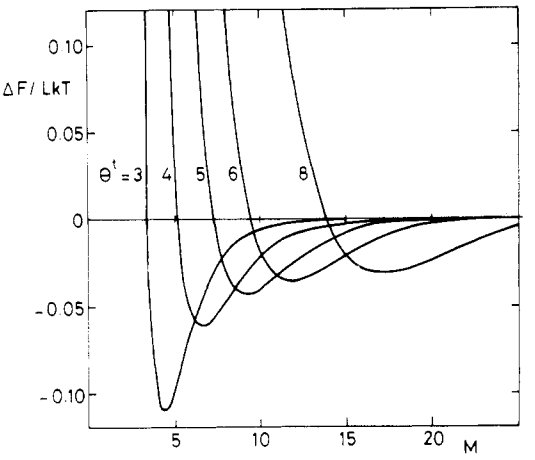

Figure 6. Interaction curves at different (constant) amounts of polymer between the surfaces (compare Figure 5). $\lambda_0 = 0.5$, $\chi = 0.7$, $\chi_s = 1$, and $r = 100$.

As we have seen in the discussion of Figure 4, the adsorption of polymer from a bulk concentration approaching the binodal has essentially no limit, since the surface acts as a nucleus for phase separation. Moreover, under these conditions there is a region of plate separations at which the free energy of interaction is independent of the plate distance, but nonzero. This applies only when full equilibrium with an infinite bulk solution can be maintained. In reality, the bulk concentration will decrease when adsorption sets in, limiting the adsorption at a certain level.

The shape of the interaction curves in restricted equilibrium at other levels than $\theta^t = 4$ is shown in Figure 6 and the corresponding segment density profiles at large plate separations ($M = 100$) are given in Figure 7. In order to reach high adsorbed amounts, the equilibrium bulk concentration at large distances has to approach the binodal. At a constant amount of polymer between the surfaces, the segment density midway between the plates must necessarily decrease with increasing plate separation, because there is no supply of polymer from the bulk solution

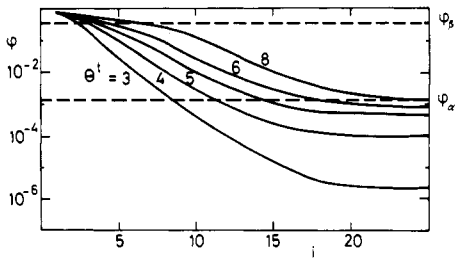

Figure 7. Segment density profiles at large plate separations (M = 100) for the systems given in Figure 6. The segment densities near one of the surfaces are plotted on a logarithmic scale. The binodal concentrations ϕ_α and ϕ_β are indicated by dashed lines.

to keep the volume fraction constant around the higher critical concentration. As a result, with increasing θ^t the minimum free energy shifts to larger separations, closely following the lowest possible equilibrium value from Figure 4 at each distance, but without the linear regions or jumps in the curves as in full equilibrium. The onset of interaction occurs approximately at a distance where $\phi_{M/2} \approx 0.01$, whereas the free energy is at its minimum when this volume fraction is somewhat lower than ϕ_β.

In practice the conditions which probably apply most often are a full equilibrium adsorption at large plate separation and a constant amount of polymer between the plates during the interaction. In Figure 8 a series of interaction curves is given for such a case. The equilibrium concentration for each curve is the same as that for the corresponding full equilibrium curve in Figure 2; i.e., $\phi_* = 10^{-6}$ except for two graphs with $\phi_* = 10^{-10}$ and $\phi_* = 10^{-2}$ in parts g and h of Figure 8. As in Figure 2, the parameters are $\lambda_0 = 0.5$, $\chi = 0.5$, $\chi_s = 1$, and $r = 1000$, unless indicated otherwise.

Nearly all interaction curves in Figure 8 show a distinct minimum. This minimum is deeper and is situated at a shorter separation if the molecular weight of the polymer is lower (see Figure 8b), mainly because of the lower adsorbed amount (Figure 8a). At this concentration (1 ppm) in a Θ-solvent the minimum occurs at $0.27r^{1/2}$ which is about 60% of the radius of gyration of a free coil in solution.

As discussed in connection with Figure 2d, a change of the adsorption energy χ_s affects the equilibrium adsorption at large plate separation (compare figures 2c and 8c) without changing the extension of the adsorbed layer very much. The result is that the interaction curves given in Figure 8d are nearly independent of χ_s.

In parts e and f of Figure 8 the effect of the solvent quality is shown. In athermal solvents ($\chi = 0$) the amount of polymer between the plates is low and hence the interaction minimum is deep and occurs at a short separation. With decreasing solvent quality this minimum shifts to larger distances while its magnitude decreases. At phase separation conditions ($\chi \approx 0.59$ at $r = 1000$ and $\phi_* = 10^{-6}$) the equilibrium adsorbed amount can increase without bounds, but the magnitude of the interaction minimum is constant (compare Figure 6 for high θ^t).

The adsorbed amount at large interplate distance (where full equilibrium applies) is a slowly increasing function of the solution concentration. However, as shown in Figure 8h, the interaction depends strongly on the amount of polymer. With increasing θ^t, the attraction decreases until at high adsorption only repulsive forces remain. This is more clearly shown in Figure 9, where we have plotted interaction curves for $r = 100$ and $r = 10\,000$ over a very wide range of adsorbed amounts.

A very interesting aspect of Figure 9 is that the interaction curves hardly depend on the molecular weight, provided that the adsorbed amount is the same. However, the equilibrium concentrations which give the same adsorbed amount at large plate separation depend very strongly on r (see the table in Figure 9). For instance, for an adsorption of 3 equivalent monolayers (1.5 monolayer

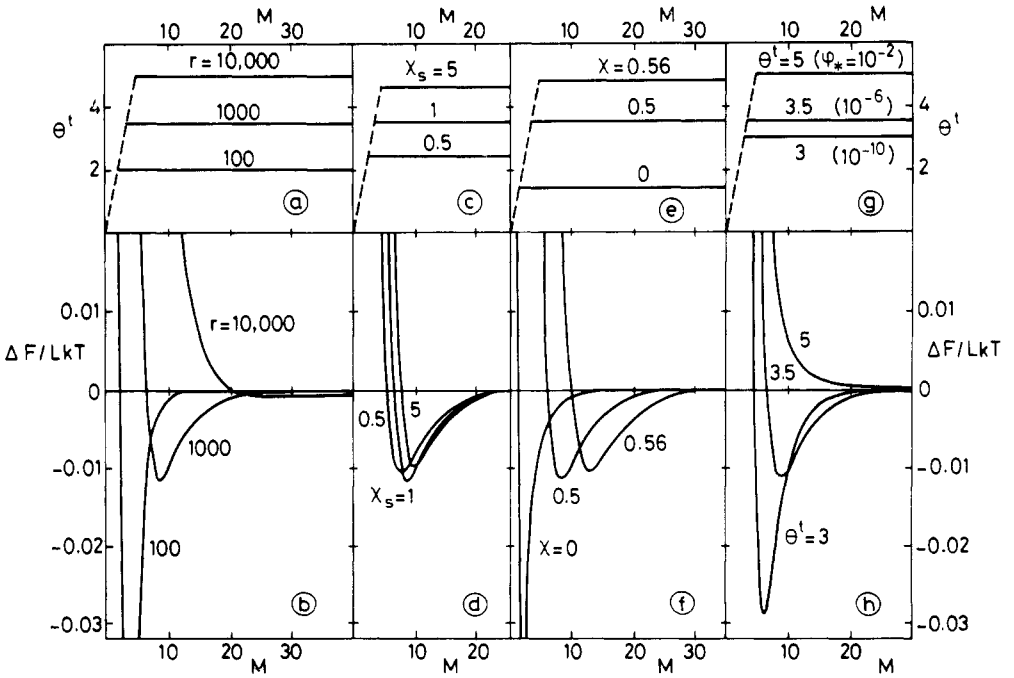

Figure 8. "Adsorption" and interaction curves at constant amounts of polymer under various conditions. The top plots show the (constant) amount of polymer between the plates and the bottom plots the free energy of interaction per surface site. In each graph the curve for $\lambda_0 = 0.5$, $\chi = 0.5$, $\chi_s = 1$, $r = 1000$, and $\theta^t = 3.5$ is given. As in Figure 2, the effect of chain length is shown in a and b, that of the adsorption energy in c and d, and that of the solvent quality in e and f, whereas curves for different amounts of polymer are given in g and h. The amount of polymer between the plates equals the equilibrium adsorption at large surface separation and $\phi_* = 10^{-6}$, except for two curves for $\phi_* = 10^{-10}$ and $\phi_* = 10^{-2}$, respectively, in graphs g and h. The minimum surface separation occurs at $M = \theta^t$, i.e., when the gap is filled with pure polymer.

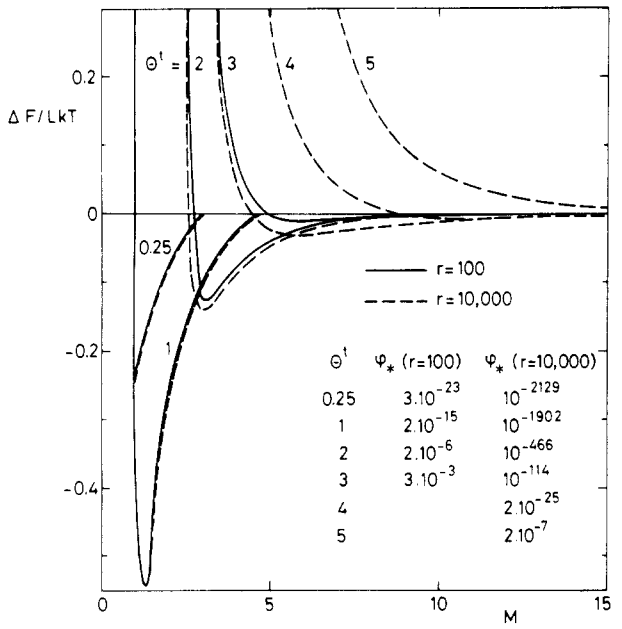

Figure 9. Interaction curves for different amounts of polymer between the surfaces, given for $r = 100$ (full curves) and $r = 10000$ (dashed curves). The corresponding equilibrium concentrations ϕ_* at large plate separations are given for each individual curve. $\lambda_0 = 0.5$, $\chi = 0.5$, and $\chi_s = 1$.

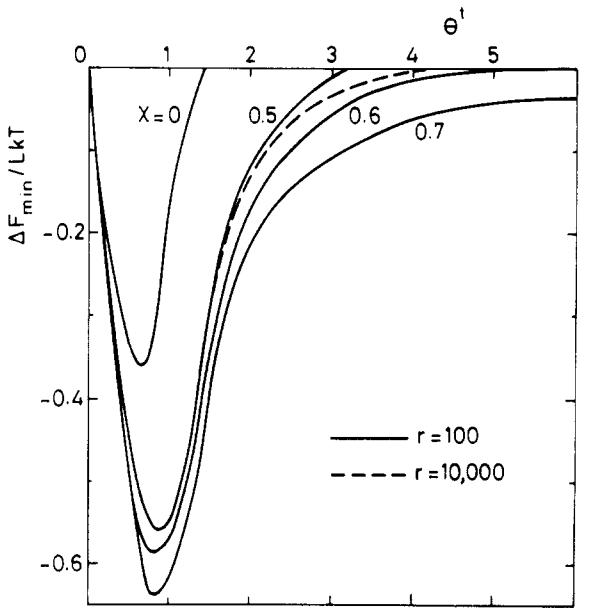

Figure 10. Free energy minimum as a function of the total amount of polymer between the surfaces for different solvent qualities. If the minimum is zero (e.g., for $\theta^t > 1.45$ at $\chi = 0$), there is only repulsion between the plates. $\lambda_0 = 0.5$, $\chi_s = 1$, $r = 100$ (full curves, for four χ values), and $r = 10000$ (dashed curves, for $\chi = 0$ and 0.5).

per plate) the equilibrium volume fractions of $r = 100$ and $r = 10000$ are 3×10^{-3} and 10^{-114}, respectively. These concentrations depend on the adsorption energy and the solvent quality, but the general trends are obvious. In order to get the same adsorbed amount, we need a high equilibrium concentration of short chains (only a part of the added polymer adsorbs), whereas for high molecular weight polymer every chain added to the system is on the surface. Since longer chains can adsorb in higher amounts, they are much better stabilizers than short chains. In Figure 9 we see that a concentration of 2 ppm of $r = 100$ gives $\theta^t = 2$ and a free energy minimum of $0.125kT$ per surface site, whereas a concentration of 0.2 ppm of $r = 10000$ gives $\theta^t = 5$ and a very strong steric stabilization. To obtain a free energy minimum of $0.125kT$ per surface site, using $r = 10000$, a total amount of 1 monolayer per plate is necessary in the system. In this case, the solution concentration is essentially zero and the adsorption is well below saturation. Consequently, the adsorbed layer is flat and tails are virtually absent; i.e., the adsorbed layer has a segment density profile independent of r.

Upon approaching of the surfaces the segment density profile between the plates becomes more homogeneous when bridges are being formed. Hence, even when the total number of segments directly adsorbed on the plates does not change, there is an attractive contribution from the increase in entropy of the chains, going from two-dimensional conformations on one surface toward conformations in which transitions between two surfaces frequently occur. Hence, we conclude that bridging is sometimes entropically favorable, in contrast to the widely held view that bridge formation decreases the entropy. Such a decrease would apply if a grafted tail adsorbs on a second surface, without rearrangements of loops, trains, and tails. The increase in entropy due to bridging is, of course, smaller for higher adsorbed amounts, when more loops and tails are present.

At very low adsorbed amounts, the free energy minimum due to adsorbed polymer again decreases, because for isolated chains the interaction between the plates is proportional to the number of molecules. In this region, the position of the minimum is at $M = 1$ and every segment is adsorbed on both of the surfaces (if a segment cannot adsorb on both surfaces at a time, the minimum depends on the structure of the chain). With increasing θ^t the depth of the interaction minimum ΔF_{min} goes through a maximum. In Figure 10 we have plotted ΔF_{min} as a function of θ^t for $\lambda_0 = 0.5$, $\chi_s = 1$, $r = 100$, and different χ values. The strongest attraction occurs when θ^t is around 0.8, hence, when the adsorption per plate is less than half a monolayer. The exact value depends slightly on the interaction parameters χ and χ_s. The interplate separation M at maximum attraction is only 1 or 2, as discussed above. From Figure 8c,d we know that χ_s affects the adsorbed amount rather than ΔF, so a rescaling of the θ^t axis in Figure 10 is sufficient to account for a different adsorption energy.

In athermal solvents ($\chi = 0$) the interaction minimum disappears around $\theta^t = 1.5$. Above this adsorbed amount only repulsion (steric stabilization) is found. With decreasing solvent quality the attraction increases and the minimum is present up to larger amounts of polymer. When $\chi = 0.6$, very close to the critical value $\chi_{cr} = 0.605$ for $r = 100$, ΔF_{min} decreases asymptotically to zero with increasing θ^t. For $\chi = 0.7$ the minimum never disappears (see also Figure 6). For comparison some curves are given for $r = 10000$. The molecular weight dependence is indeed very low provided that a comparison is made at the same θ^t, hence, at widely different solution concentrations. For athermal solvents, the curves for $r = 100$ and $r = 10000$ virtually coincide. For $\chi = 0.5$ there is some chain length dependence at high adsorbed amounts, mainly because the critical χ value decreases with increasing chain length. For instance, for $r = 10000$ the attraction minimum will not disappear when $\chi > 0.51$.

C. Comparison with Results of Other Theories. Results for the interaction between two adsorbed layers in full equilibrium with a bulk solution are given by Mackor and van der Waals[30] and Ash and Findenegg.[9] These authors found repulsion for adsorption of *asymmetric* dimers and tetramers. For oligomers with every segment of the same type, Ash and Findenegg found an

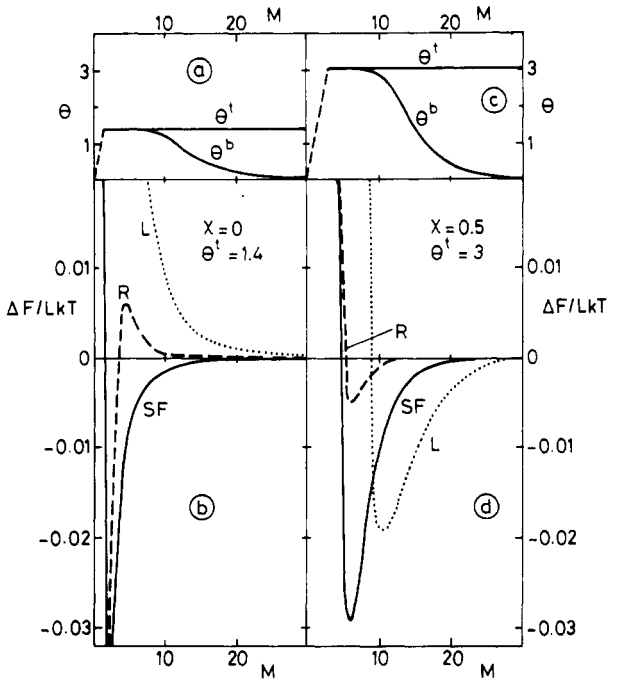

Figure 11. Comparison between interaction curves (bottom plots (b and d)) according to various theories. Full curves correspond to the present theory (SF), dashed curves to that of Roe (R), and dotted curves to that of Levine et al. (L). The top plots (a and c) give the total amount of polymer θ^t and in addition the contribution of bridging polymer θ^b as derived from the present theory. All curves have been calculated by the present authors. In order to show more clearly the effect of the osmotic term, we have used $\langle\phi_i\rangle$ instead of ϕ_i in Levine's equations where appropriate. Thus, the SF and L curves are based on the same segment density profiles. $\lambda_0 = 0.5$, $\chi_s = 1$, $r = 1000$; a and b: $\chi = 0$, $\theta^t = 1.4$; c and d: $\chi = 0.5$, $\theta^t = 3$.

attractive force between the plates. A quantitative comparison with this latter result is possible, because their model reduces to ours for $z \to \infty$ and a previous comparison of the adsorption isotherms showed quantitative agreement.[23] We have recalculated Figure 2 of ref 9 using our model and found nearly the same shape of the interaction curves, for both dimers and tetramers in different solvents, but with the free energy a factor of 2 lower. We expect a mistake in their free energy axis, because a transition from $z = 12$ to $z \to \infty$ cannot explain such a large difference. Especially for dimers in athermal solvents the same result should have been found.

We concluded already in section VI.A that the prediction of de Gennes that in full equilibrium always attraction occurs agrees with our results.

For restricted equilibrium a quantitative comparison is possible with the free energy equation of Levine et al.[36] and with that of Roe.[10] The latter theory has been developed for adsorption on one plate, but the application to two plates is straightforward. Figure 11 shows adsorption (top) and interaction curves (bottom), both for $\chi = 0$ (left) and $\chi = 0.5$ (right). The top diagrams (Figure 11a,c) give also the amount of bridging polymer. The interaction curves (Figure 11b,d) are given according to the theories of Levine et al. (L), Roe (R), and Scheutjens and Fleer (SF).

As discussed in section III.B, Levine et al. used ϕ_i instead of $\langle\phi_i\rangle$ for the fraction of polymer segments around a site in layer i and used a free energy expression in which, implicitly, the osmotic term $-\sum(\ln \phi_i^\circ + \chi\phi_i\langle\phi_i\rangle)$ occurs twice. For $\chi = 0$ the osmotic force is always repulsive (note that $-\sum\ln \phi_i^\circ = \theta^t + \sum {}^1/_2\phi_i^2 + \ldots$ and θ^t is constant). A comparison of the dotted curve and the full curve in Figure 11b makes it possible to split up the total free energy of interaction in the osmotic term and the free energy due to bridging. The difference between dotted and full curve is just the term $-\sum\ln \phi_i^\circ$ + constants. This difference is much larger than the total interaction energy according to the full curve, which is the sum of the positive osmotic term and the negative bridging term. Hence, the osmotic repulsion and the attraction due to bridging largely compensate each other. In this case the (small) difference results in an interaction curve with a minimum at $M \approx 2$. We have shown in Figure 9 that this minimum disappears at a higher adsorbed amount. The onset of the osmotic repulsion and the bridging attraction at $M \approx 30$ in Figure 11b corresponds with the appearance of bridges at that plate separation in Figure 11a.

The dashed curve in Figure 11b represents the interaction curve as predicted by the Roe theory. Due to the neglect of tails in this theory, the segment density profile is much steeper. The result is that the onset of bridging occurs at a smaller plate separation than the onset of the osmotic repulsion between the loop layers, giving rise to a free energy barrier. We have shown in section III.A that no difference exists between Roe's theory and ours for $M = 1$. In Figure 11b we see that the curves deviate strongly at $M > 1$. This difference in ΔF arises from the fact that the free energy is very sensitive to small variations in the profile. A consequence is that also the free energy of the reference state (at large plate separations) is different. Despite this problem the existence of a minimum in the interaction free energy in good solvents is fully corroborated, also in Roe's model.

Parts c and d of Figure 11 give the results for $\chi = 0.5$. The adsorption is much higher and the position of the free energy minimum is shifted to larger plate separations. For the curve from Levine's equations we have used the more correct form $\chi\phi_i\langle\phi_i\rangle$ instead of $\chi\phi_i^2$; i.e., we have used the same segment density profile for the Levine (L) and Scheutjens–Fleer (SF) curves. The approximate osmotic term $-\sum(\ln \phi_i^\circ + \chi\phi_i^2)$ is always repulsive for $\chi \leq 0.5$, but the more correct form $-\sum(\ln \phi_i^\circ + \chi\phi_i\langle\phi_i\rangle)$, which is the difference between the dotted curve and the full curve in Figure 11d (apart from a constant), gives a strong attractive contribution in the region between $M = 10$ and $M = 30$. However, this contribution is compensated by a bridging term which is in this case *repulsive* unlike at $\chi = 0$. For the region between $M = 5$ and $M = 10$ the (correct) osmotic term is repulsive and the bridging term strongly attractive. The dashed curve in Figure 11d shows that in this case the Roe theory predicts a small minimum without a free energy barrier. The absence of the barrier is probably related to the decreasing steepness of the segment density profile with increasing χ.

A qualitative comparison with results from the Cahn–de Gennes approach shows that there are some discrepancies. At constant amount of polymer, de Gennes[38] found only repulsive forces in good solvents. The free energy at large plate separations varies as M^{-2} and at small separations as $M^{-5/4}$. These predictions are confirmed by experimental results of Klein and Luckham.[50] We have not yet examined the strong repulsive forces at small separations but find a minimum in the free energy whenever the adsorbed amount is lower than a critical value, and in poor solvents there is always a free energy minimum. Klein and Pincus,[40] using the same type of analysis, found attraction in poor solvents when the segment density between the surfaces is in the instable region given by the binodal. They have predicted that the segment density profiles in poor solvents exhibit three regions: The density falls

rapidly to ϕ_β over a distance z_0, traverses slowly the unstable region between ϕ_β and ϕ_α (broad central plateau from z_0 to $2z_0$), and falls exponentially toward the bulk concentration. As in our results, the minimum free energy of interaction occurs when the volume fraction midway between the plates is near ϕ_β. The segment density profiles in Figure 7 do not show such a plateau region: on a logarithmic scale the decay in the unstable region is faster than in the initial part and no irregularities occur near ϕ_α.

As discussed before, the model of de Gennes neglects end effects, which are responsible for the difference between the R and SF curves in Figure 11. However, this cannot be the only reason for the discrepancy, since also the Roe theory predicts attraction in good solvents at low adsorbed amounts of polymer.

D. Comparison with Experimental Data. Currently, the only suitable experimental data for testing the theory are those of Klein and co-workers.[41,42,45,46,50,51] Their results show reversible interaction curves which all exhibit repulsive forces at very short plate separation. Hence the amount of polymer between the plates probably does not change during compression. We will assume a restricted equilibrium. Qualitatively, all data support the results given in Figures 8 and 9; i.e., there is a minimum in the free energy at a distance comparable to the radius of gyration of a free coil in solution and this minimum is deeper for poorer solvents and lower adsorbed amounts. The minimum disappears for high adsorbed amount in good solvents.[45,46] For a quantitative comparison, the knowledge of the adsorbed amount of polymer would be necessary. However, the reported values are rather uncertain and sometimes contradicting. For instance, in one case the average volume fraction of polystyrene between the mica surfaces was 25% at a distance of 20 nm and 100% at 12 nm,[51] i.e., an increase in adsorbed amount of 140% upon compression by less than a factor 2. These uncertainties make a quantitative comparison, as yet, impossible.

In our analysis of the theoretical data, we found, with varying θ^t, a linear relation between ΔF_{min} and M_{min}^{-2}, such that $(\Delta F_{min} - A)M_{min}^2 = B$, where A is a positive constant for good solvents, zero for Θ solvents, and negative for poor solvents. The value of B does not depend on χ and χ_s, varies slightly with r, and is nearly proportional to the lattice constant λ_1. For $\lambda_1 = 0.25$ ($\lambda_0 = 0.5$), B is around $-1.8kT$ for $r = 100$ and $B \approx -1.4\ kT$ for $r = 1000$. The advantage of using B is that it is independent of the scaling of a lattice layer, surface site, or segment length. Some experimental data of Klein et al. indicate a B value between $-20kT$ and $-50kT$, so that possibly our free energy minima are 1 order of magnitude too low. The number of available experimental interaction curves for various amounts of polymer is too small for a test on the linearity between ΔF_{min} and M_{min}^{-2}.

VII. Conclusions

On the basis of a previously developed lattice model for polymer adsorption, the interaction free energy between two adsorbed polymer layers is derived.

At full equilibrium, when the polymer can freely enter and leave the gap between the surfaces, the interaction is always attractive. The minimum free energy occurs when a monolayer of polymer chains in strictly two-dimensional conformations is sandwiched between the surfaces. A practical consequence might be that stabilization of liquid films by adsorbing homopolymers is impossible.

If the polymer cannot enter or leave the gap during the time of interaction, the interaction force is attractive at large distances and repulsive at short distances. The attraction is due to bridging of the chains between the opposing walls. In poor solvents an additional osmotic contribution to the attraction exists up to very large distances. The minimum free energy is only slightly above the free energy at full equilibrium at the same plate separation. The attraction is strong for low adsorbances, i.e., for low molecular weight polymer or at low concentrations. This effect explains the bridging flocculation, which is often observed experimentally.

The interaction is determined by the adsorbed amount rather than by the solution concentration or molecular weight. The range of adsorbed amounts at which flocculation may occur decreases with solvent quality. The strongest attraction occurs when the adsorbance on each surface is slightly below 0.5 segments per surface site. However, this strong minimum occurs at a short distance. For a given system, the minimum free energy is nearly inversely proportional to the square of the distance at which it occurs.

At high adsorbed amount the free energy minimum is absent (except in poor solvents) and a strong repulsion occurs. However, in order to obtain a high adsorbed amount, a much higher solution concentration of low molecular weight polymer is required than for longer chains. Hence, at the same solution concentration, high molecular weight polymer is a much better stabilizer.

Comparison with available experimental data of Klein et al. reveals that all predictions agree qualitatively, whereas quantitatively the position of the minimum free energy is correct, but its value is possibly 1 order of magnitude too low. Nevertheless, we have presented the first prediction that both bridging attraction and steric stabilization are possible in good solvents as well.

Appendix I. Comparison with the Roe Model

The identity of our eq 23 and Roe's eq 36 can be shown as follows. Shift all terms of eq 29 of ref 10 to the left-hand side and call the sum of these terms zero(i), which is zero. Then add $\sum\phi_i$ zero(i) to his eq 36 for the surface tension and after some rearrangement our eq 23 appears. In doing so, one must realize that $\sum\phi_i\langle\phi_i/\langle\phi_i\rangle\rangle = \sum\langle\phi_i\rangle\phi_i/\langle\phi_i\rangle = \sum\phi_i$.

A similar rearrangement is possible for Roe's eq 36′, representing the surface tension of a multicomponent mixture. For such a system the last two terms of eq 13 are to be replaced by $-\sum_x\{n^x \ln r^x - (r^x - 1)n^x \ln L\}$ and the interaction energy is $-\sum_x\chi_s{}^x(n_1{}^x + n_M{}^x) + {}^1/_2\sum_i\sum_x\sum_y\chi^{xy}n_i{}^x(\phi_i{}^y)$, where x and y are the component indices. The double summation over x and y extends over all components, including solvent. By definition $\chi^{xx} = 0$. Differentiation of $-kT \ln Q$ with respect to L and addition of $\mu^\circ M$ gives eq 25. This equation (without the factor 2) follows from Roe's eq 36′ after addition of $\sum_i\sum_x\phi_i{}^x(\Psi_i{}^\circ - \Psi_i{}^x)$, where $\Psi_i{}^x$ is given by Roe's eq 41.

Appendix II. Comparison with Other Theories for Restricted Equilibrium

1. DiMarzio and Rubin.[13] For $n = 1$, eq 24 reduces to $F - F^\circ + kT \ln (L/r) = -kT \ln P(r)$, which is the free energy equation used by DiMarzio and Rubin.[13] For a single chain ($\phi_i \to 0$ and $\phi_s \to 1$) and athermal conditions ($\chi = 0$) our weighting factors P_i are identical with their factors $\exp(\theta_i)$.

2. Meier[31] and Hesselink.[32,33] For a system of nonadsorbing, terminally attached chains (or loops, tails) these authors use a volume restriction terrm $-kT(n/L) \ln (\sum\omega_c)$ and an osmotic term $kT({}^1/_2 - \chi)\sum\phi_i{}^2$. This is consistent with eq 24, provided that all weighting factors P_i are equal. Then we may approximate $(n/L) \ln P(r) \simeq (n/L) \ln \sum\omega_c + \sum\phi_i \ln P_i$ (see eq 22). Substitution into eq 24 gives

immediately eq 26. A Taylor expansion of $-\sum\phi_i \ln P_i \simeq \chi\theta^t - \sum\{2\chi\phi_i^2 + \phi_i \ln (1 - \phi_i)\}$, retaining terms up to order ϕ_i^2, gives $\chi\theta^t + 2(^1/_2 - \chi)\sum\phi_i^2$. Similarly, the last two terms of eq 26 can be approximated by $-\theta^t - (^1/_2 - \chi)\sum\phi_i^2$ when $\langle\phi_i\rangle$ is replaced by ϕ_i. Since θ^t is constant, we may conclude that the sum of the last three terms represents Hesselink's osmotic term apart from a constant. It is interesting to observe that the term $-(n/L) \ln P(r)$ contains twice the osmotic term $(^1/_2 - \chi)\sum\phi_i^2$ of Hesselink. The last two terms of eq 24 constitute a correction for one of them. Neglecting this correction (as Levine did) overestimates the osmotic term by a factor of about 2.

3. Dolan and Edwards.[34] We rewrite the last two terms of eq 26 as $(^1/_2\chi - 1)\theta^t + {}^1/_2\sum\phi_i \ln P_i$. Addition of the second term $(-\sum\phi_i \ln P_i)$ and combination with the first term gives $F - F^\circ \simeq -nkT \ln (\sum_c \omega_c \prod_i P_i^{r_{i,c}/2}) +$ constants. In the term $-(n/L) \ln P(r)$ as used by Dolan and Edwards, P_i is replaced by $P_i^{1/2}$; hence the osmotic term occurs only once in their expression and correction terms are not necessary in their free energy function.

4. Levine, Thomlinson, and Robinson.[36] These authors adopted the free energy function $-kTn \ln P(r)$, probably taken from DiMarzio and Rubin[13] or Dolan and Edwards,[34] and thus missed the middle two terms of eq 24, which are approximately zero in the latter theories. Note that $-\sum \ln \phi_i^\circ$ is infinite for pure polymer between the plates ($\phi_i^\circ \to 0$), whereas the free energy must remain finite (compare eq 26 for $\phi_i^\circ \to 0$). In fact, for pure polymer $P_i = 0$ and therefore $-n \ln P(r)$ is infinite as well, compensating the sum $\sum \ln \phi_i^\circ$ in eq 24. Since this compensation is absent in Levine's equation, his free energy function is qualitatively wrong.

Appendix III. Glossary

A	surface area per plate; constant (section VI.D)
a	A/L, area per lattice site
B	constant (section VI.D)
C	normalization constant (eq 20 and 21)
c, d	specification for chain conformation
F, F°	free energy of the mixed system and of pure solvent between the plates, respectively
ΔF	$F(M) - F(\infty)$, free energy of the system at plate separate M with respect to that at large plate separations (restricted equilibrium)
ΔF_{min}	minimum of $\Delta F(M)$, i.e., ΔF at zero force
G	specification for group of chains; G is f (free), a′ (adsorbed on plate 1 only), a″ (adsorbed on plate 2 only), b′ (bridging and last tail on plate 1), b″ (bridging and last tail on plate 2), or b (=b′ + b″)
i, j	layer number
k	Boltzmann's constant
L	number of lattice sites per layer
$l^{G,S}$	average length of subchains S in chain group G
M	number of lattice layers (plate separation)
M_{min}	plate separation at minimum free energy (zero force)
n, n°	number of chains and solvent molecules, respectively, between the plates
n_c, n_d	number of chains in conformations c and d, respectively
$\{n_c\}$	distribution of chain conformations
n_i, n_i°	number of segments and solvent molecules, respectively, in layer i
n_i^x	number of segments (or solvent molecules) of type x in layer i
n^b	number of bridges per bridging chain
$n^{G,S}$	number of subchains S per chain of group G
$n^{G,S}(s)$	number of subchains S, s segments long, per chain of group G
P_i, P_*	segmental weighting factor in layer i and in the bulk solution, respectively
$P(i,s)$	weight of all s-mers having segment s in layer i
$P^G(i,s)$	weight of all s-mers in group G having segment s in layer i
$P(r)$	$\sum_i P(i,r)$ weight of all chains of r segments
$P^G(r)$	weight of all chains of r segments in group G
$\langle P(i,s)\rangle$	$\lambda_1 P(i-1,s) + \lambda_0 P(i,s) + \lambda_1 P(i+1,s)$
$Q(\{n_c\}, V,A,T)$	partition function for a given distribution of conformations
Q_+, Q_+°	partition function for n chains in pure polymer and for n° solvent molecules in pure solvent, respectively
q	number of chemical bonds parallel to the surface of a chain in a given conformation
r	number of segments per chain
r^x	number of segments per chain of type x
$r_{i,c}, r_{i,d}$	number of segments that a chain in conformations c and d, respectively, has in layer i
S	specification for subchains: S is either b (bridge), l (loop), t (tail), or tr (train)
s	segment ranking number; length of a subchain
T	absolute temperature
V	volume between the plates
X_i	$\ln P_i$ (iteration variable)
x, y	specification for segment or solvent type in a mixture
z	coordination number of the lattice
γ, γ°	surface tension of the mixed system ($2\gamma = \gamma' + \gamma''$) and of pure solvent, respectively
γ', γ''	surface tension at plate 1 and at plate 2, respectively
$\Delta\gamma$	$2\gamma(M) - 2\gamma(\infty)$, free energy of the system at plate separation M with respect to that at large plate separations (full equilibrium)
$\delta_{i,j}$	Kronecker delta, $\delta_{i,j} = 1$ if $i = j$ and $\delta_{i,j} = 0$ otherwise
$\delta(r)$	correction term for odd number of segments per chain (section V)
Θ solvent	ideally poor solvent ($\chi = 0.5$)
θ	adsorbed amount expressed as the number of equivalent monolayers
θ^{exc}, θ^t	excess amount and total amount of polymer between the plates, respectively ($\theta^{exc} = \theta^t - M\phi_*$, $\theta^t = \sum\phi_i$)
$\theta^{x,exc}$	excess amount of component x
θ^b, θ^G	amount of bridging polymer and of polymer in group G, respectively
θ_i	$\exp(\chi_s\delta_{1,i})$, energy parameter in DiMarzio–Rubin theory (Appendix II)
κ	constant in gradient term of Cahn–de Gennes theory
λ_0, λ_1	fraction of nearest neighbors in the same layer and in each of the adjacent layers, respectively
λ_{i-j}	fraction of nearest neighbors in layer j around a site in i
μ, μ°	chemical potential of a chain and of a solvent molecule, respectively, with respect to the reference state
$\nu^{G,S}$	fraction of segments in subchains S of group G
Ξ	grand partition function of the system at full equilibrium

ϕ_i, ϕ_* volume fraction of segments in layer i and in the bulk solution, respectively

ϕ_i°, ϕ_*° volume fraction of solvent in layer i and in the bulk solution, respectively

$\langle\phi_i\rangle$, $\langle\phi_i^\circ\rangle$ average volume fraction of segments and of solvent molecules, respectively, around a site in layer i

$\phi_i(s)$ volume fraction of segments s in layer i

ϕ_i^G volume fraction of polymer group G in layer i

$\phi_i^G(s)$ volume fraction of segments s of group G in layer i

$\phi_i^{G,S}$ volume fraction of subchains S of group G in layer i

ϕ_i^x, ϕ_i^y volume fraction of segment type x and y, respectively, in layer i

ϕ_*^x, ϕ_*^y volume fraction of segment type x and y, respectively, in the bulk solution

ϕ_{cr} volume fraction of polymer at the critical point

ϕ_α, ϕ_β volume fraction of polymer in the dilute phase and in the concentrated phase, respectively, after phase separation

ϕ_α°, ϕ_β° volume fraction of solvent in the dilute polymer phase and in the concentrated polymer phase, respectively, after phase separation

χ Flory–Huggins polymer–solvent interaction parameter

χ^{xy} Flory–Huggins interaction parameter between segments (or solvent) of type x and type y

χ_{cr} χ at the critical point of the phase diagram

χ_s differential adsorption energy per segment with respect to solvent

χ_s^x differential adsorption energy per segment of type x

Ψ partition function of the system between the plates at constant amount of polymer

Ψ_i^x, Ψ_i° energy function in Roe's theory for component x and for solvent, respectively, in layer i (Appendix I)

$\Omega(\{n_c\})$ combinatory factor for a given distribution of conformations

Ω_+ combinatory factor for n polymer chains in amorphous bulk polymer

ω_c, ω_d ratio between the number of arrangements of a chain in conformations c and d, respectively, and that of a chain in bulk polymer

References and Notes

(1) Vincent, B. *Adv. Colloid Interface Sci.* **1974**, *4*, 193.
(2) Tadros, T. F. In "The Effect of Polymers on Dispersion Properties"; Tadros, T. F., Ed.; Academic Press: London, 1982; p 1.
(3) Yarar, B. In "Solution Behavior of Surfactants"; Mittal, K. L., Fendler, E. J., Eds.; Plenum Press: New York, 1982; Vol. 2, p 1333.
(4) Kitchener, J. A. *Br. Polym. J.* **1972**, *4*, 239.
(5) Somasundaran, P. In "Fine Particles Processing"; Somasundaran, P., Ed.; AIME: New York, 1980; Vol. 2.
(6) Silberberg, A. *J. Chem. Phys.* **1968**, *48*, 2835.
(7) Hoeve, C. A. J. *J. Chem. Phys.* **1966**, *44*, 1505.
(8) Ash, S. G.; Everett, D. H.; Findenegg, G. H. *Trans. Faraday Soc.* **1970**, *66*, 708.
(9) Ash, S. G.; Findenegg, G. H. *Trans. Faraday Soc.* **1971**, *67*, 2122.
(10) Roe, R. J. *J. Chem. Phys.* **1974**, *60*, 4192.
(11) Scheutjens, J. M. H. M.; Fleer, G. J. *J. Phys. Chem.* **1979**, *83*, 1619.
(12) DiMarzio, E. A. *J. Chem. Phys.* **1965**, *42*, 2101.
(13) DiMarzio, E. A.; Rubin, R. J. *J. Chem. Phys.* **1971**, *55*, 4318.
(14) de Gennes, P.-G. *Macromolecules* **1980**, *13*, 1069.
(15) de Gennes, P.-G. *Macromolecules* **1981**, *14*, 1637.
(16) de Gennes, P.-G. *Phys. Lett. A* **1972**, *38*, 339.
(17) Clark, A. T.; Lal, M. *J. Chem. Soc., Faraday Trans. 2* **1981**, *77*, 981.
(18) Clark, A. T.; Lal, M. In "The Effect of Polymers on Dispersion Properties"; Tadros, T. F., Ed.; Academic Press: London, 1982; p 169.
(19) Feigin, R. I.; Napper, D. H. *J. Colloid Interface Sci.* **1980**, *75*, 525.
(20) Hoeve, C. A. J. *J. Polym. Sci., Part C* **1970**, *30*, 361.
(21) Hoeve, C. A. J. *J. Polym. Sci. Part C* **1971**, *34*, 1.
(22) Scheutjens, J. M. H. M.; Fleer, G. J. *J. Phys. Chem.* **1980**, *84*, 178.
(23) Scheutjens, J. M. H. M.; Fleer, G. J. In "The Effect of Polymers on Dispersion Properties"; Tadros, T. F., Ed.; Academic Press: London, 1982; p 145.
(24) Fleer, G. J.; Scheutjens, J. M. H. M. *Adv. Colloid Interface Sci.* **1982**, *16*, 341.
(25) Barnett, K.; Cosgrove, T.; Crowley, T. L.; Tadros, T. F.; Vincent, B. In "The Effect of Polymers on Dispersion Properties"; Tadros, T. F., Ed.; Academic Press: London, 1982; p 183.
(26) Cosgrove, T.; Vincent, B.; Crowley, T. L.; Cohen Stuart, M. A. *ACS Symp. Ser.* **1984**, *No. 240*, 147.
(27) Cohen Stuart, M. A.; Scheutjens, J. M. H. M.; Fleer, G. J. *J. Polym. Sci., Polym. Phys. Ed.* **1980**, *18*, 559.
(28) Mackor, E. L. *J. Colloid Sci.* **1951**, *6*, 492.
(29) Dolan, A. K.; Edwards, S. F. *Proc. R. Soc., London, Ser. A* **1974**, *337*, 509.
(30) Mackor, E. L.; van der Waals, J. H. *J. Colloid Sci.* **1952**, *7*, 535.
(31) Meier, D. J. *J. Phys. Chem.* **1967**, *71*, 1861.
(32) Hesselink, F. T. *J. Phys. Chem.* **1971**, *75*, 65.
(33) Hesselink, F. T.; Vrij, A.; Overbeek, J. T. G. *J. Phys. Chem.* **1971**, *75*, 2094.
(34) Dolan, A. K.; Edwards, S. F. *Proc. R. Soc. London, Ser. A* **1975**, *343*, 427.
(35) Gerber, P. R.; Moore, M. A. *Macromolecules* **1977**, *10*, 476.
(36) Levine, S.; Thomlinson, M. M.; Robinson, K. *Discuss. Faraday Soc.* **1978**, *65*, 202.
(37) Flory, P. J. "Principles of Polymer Chemistry"; Cornell University Press: Ithaca, NY, 1953.
(38) de Gennes, P.-G. *Macromolecules* **1982**, *15*, 492.
(39) Cahn, J. *J. Chem. Phys.* **1977**, *66*, 3667.
(40) Klein, J.; Pincus, P. *Macromolecules* **1982**, *15*, 1129.
(41) Klein, J. *Nature (London)* **1980**, *288*, 248.
(42) Klein, J. *Adv. Colloid Interface Sci.* **1982**, *16*, 101.
(43) Scheutjens, J. M. H. M.; Fleer, G. J. *Adv. Colloid Interface Sci.* **1982**, *16*, 361.
(44) Scheutjens, J. M. H. M.; Fleer, G. J. *Adv. Colloid Interface Sci.* **1983**, *18*, 309.
(45) Israelachvili, J. N.; Tirrell, M.; Klein, J.; Almog, Y. *Macromolecules* **1984**, *17*, 204.
(46) Klein, J.; Luckham, P. *Nature (London)* **1984**, *308*, 836.
(47) Gaylord, R. J. *J. Colloid Interface Sci.* **1982**, *87*, 577.
(48) Helfand, E.; Sapse, A. M. *J. Chem. Phys.* **1975**, *62*, 1327.
(49) Powell, M. J. D. In "Numerical Methods for Nonlinear Algebraic Equations"; Rabinowitz, P., Ed.; Gordon and Breach: London, 1970; pp 87, 115.
(50) Klein, J.; Luckham, P. F. *Macromolecules* **1984**, *17*, 1041.
(51) Klein, J.; Almog, Y.; Luckham, P. *ACS Symp. Ser.* **1984**, *No. 240*, 227.